Modern Methods in Heterogeneous Catalysis Research

Permittivity and Conductivity Measurements

12th November 2010

Maik Eichelbaum / FHI

Motivation

Motivation

The p-type semiconductor $(VO)_2P_2O_7$: active phase in selective butane oxidation to maleic anhydride

n-butane → maleic anhydride

$$C_4H_{10} + 7/2\ O_2 \xrightarrow{VPO} C_4H_2O_3 + 4\ H_2O$$

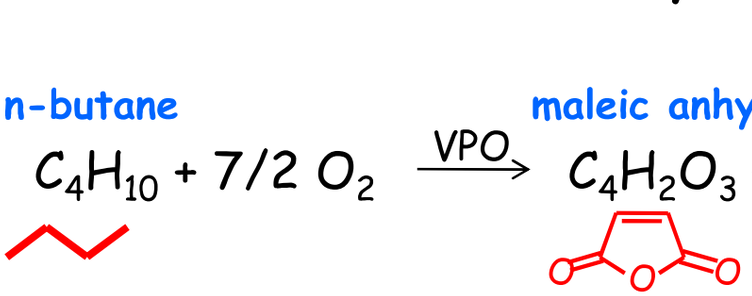

1st step: Oxydehydrogenation of butane to butene:

$$C_4H_{10} + 2h^{\cdot} + O_o^{x} \rightarrow C_4H_8 + H_2O + V_O^{\cdot\cdot}$$

Regeneration of holes: $\frac{1}{2}O_2(g) + V_O^{\cdot\cdot} \rightarrow O_o^{x} + 2h^{\cdot}$

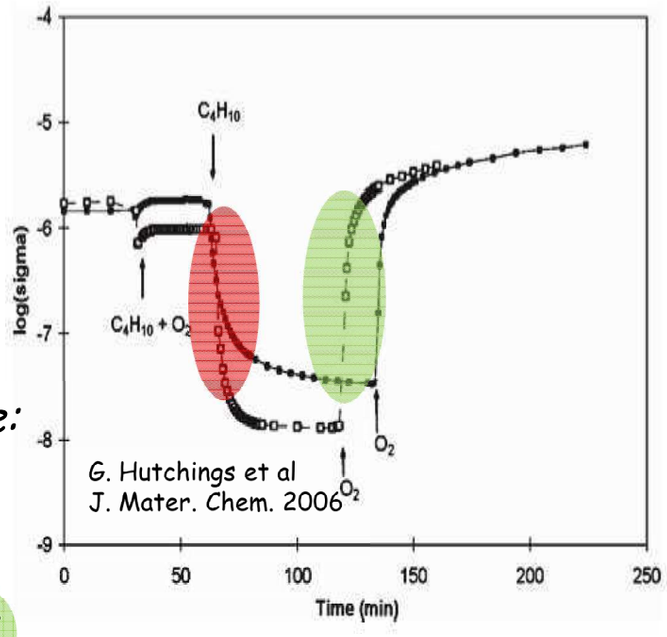

"Chemical translation": $V^{5+} + O^{2-} \rightarrow V^{4+} + O^{-}$

$O^{-} = O^{2-} + h^{+}$

Motivation

Catalysis Today xxx (2010) xxx–xxx

Contents lists available at ScienceDirect

Catalysis Today

journal homepage: www.elsevier.com/locate/cattod

Electrical conductivity of a MoVTeNbO catalyst in propene oxidation measured in operando conditions

M. Caldararu [a,*], M. Scurtu [a], C. Hornoiu [a], C. Munteanu [a], T. Blasco [b,**], J.M. López Nieto [b]

[a] Institute of Physical Chemistry "Ilie Murgulescu" of the Romanian Academy, Spl. Independentei 202, 060021 Bucharest, Romania
[b] Instituto de Tecnología Química, UPV-CSIC, Campus Universidad Politécnica de Valencia, Avda. Los Naranjos s/n, 46022 Valencia, Spain

- For semiconducting n-type metal oxides exposure to **oxygen** induces a **reduced conductivity** due to electron trapping:

$$O_{2(gas)} + e \leftrightarrow O_2^- + e \leftrightarrow 2O^-$$

- Interaction with a **reducing gas** (e.g. propene) → **conductivity increase** due to formation of anion vacancies: (or consumption of oxygen ad-ions):

$$O_{(lattice)} + \text{hydrocarbon} \rightarrow \text{oxidation products} + V_O$$

Motivation

23962 J. Phys. Chem. B 2006, 110, 23962−23967

Mechanism of the Oxidation−Reduction of the MoVSbNbO Catalyst: In Operando X-ray Absorption Spectroscopy and Electrical Conductivity Measurements

Olga V. Safonova,† Benoit Deniau,‡ and Jean-Marc M. Millet*,‡

European Synchrotron Radiation Facility, 6 rue Jules Horowitz, 38043 Grenoble Cedex, France, and Institut de Recherches sur la Catalyse CNRS conventionné avec l'Université Claude Bernard, Lyon I, 2 avenue A. Einstein, 69626 Villeurbanne Cedex, France

Received: July 11, 2006; In Final Form: September 8, 2006

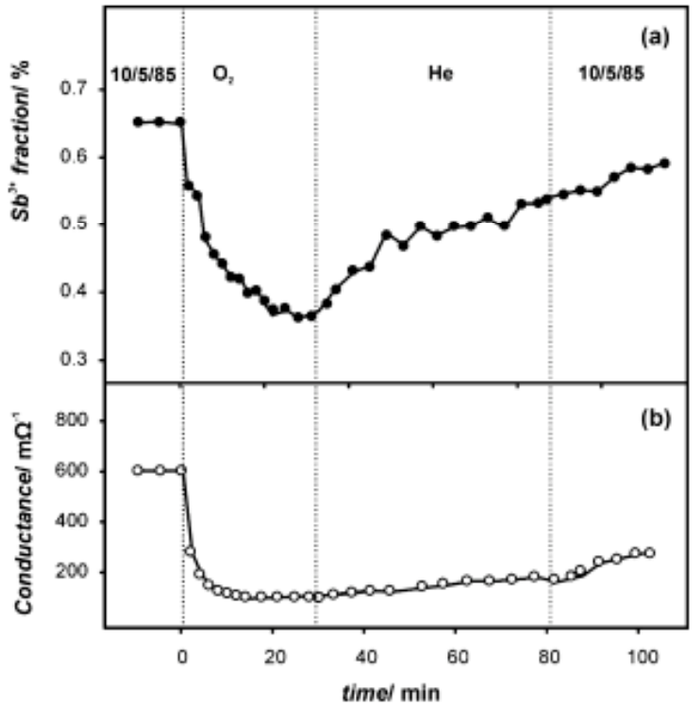

Figure 6. Kinetics of oxidation and reduction of antimony and the variation in electrical conductance of the M1 phase at 380 °C.

Motivation

The Effect of Oxygen-Anion Conductivity of Metal–Oxide Doped Lanthanum Oxide Catalysts on Hydrocarbon Selectivity in the Oxidative Coupling of Methane

Holger Borchert¤ and Manfred Baerns†

Lehrstuhl für Technische Chemie, Ruhr-Universität Bochum, D-44780 Bochum, Germany

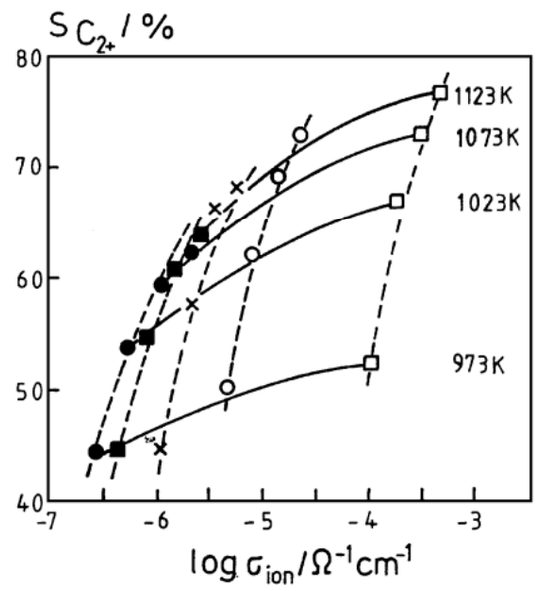

FIG. 7. C_{2C} selectivity of La_2O_3 and Me^{nC} (1 at-%)/La_2O_3 catalysts in dependence on oxygen-anion conductivity. (Reaction conditions: $P^{\pm}_{CH_4}$ D 60 kPa, $P^{\pm}_{O_2}$ D 6 kPa, $P^{\pm}_{N_2}$ D 34 kPa, $X_{O_2} > 90\%$.) Symbols Me^{nC} : Zn^{2C} (○), Sr^{2C} (□), Ti^{4C} (●), Nb^{5C} (■); La_2O_3 (£).

Motivation

10554 *J. Phys. Chem. C* **2009,** *113,* 10554–10559

Understanding the Dielectric Properties of Heat-Treated Carbon Nanofibers at Terahertz Frequencies: a New Perspective on the Catalytic Activity of Structured Carbonaceous Materials

Edward P. J. Parrott,[†,‡] J. Axel Zeitler,[‡] James McGregor,[‡] Shu-Pei Oei,[§] Husnu Emrah Unalan,[§] Swee-Ching Tan,[¶] William I. Milne,[§] Jean-Philippe Tessonnier,[∥] Robert Schlögl,[∥] and Lynn F. Gladden*[,‡]

Department of Physics, Cavendish Laboratory, University of Cambridge, J. J. Thomson Avenue, Cambridge CB3 0HE, United Kingdom, Department of Chemical Engineering and Biotechnology, University of Cambridge, Pembroke Street, Cambridge CB2 3RA, United Kingdom, Centre for Advanced Photonics and Electronics, University of Cambridge, J. J. Thomson Avenue, Cambridge CB3 0FA, United Kingdom, University of Cambridge Nanoscience Centre, J. J. Thomson Avenue, Cambridge CB3 0FF, United Kingdom, and Fritz-Haber-Institut der Max-Planck-Gesellschaft, Berlin D-14195, Germany

Received: December 19, 2008; Revised Manuscript Received: April 24, 2009

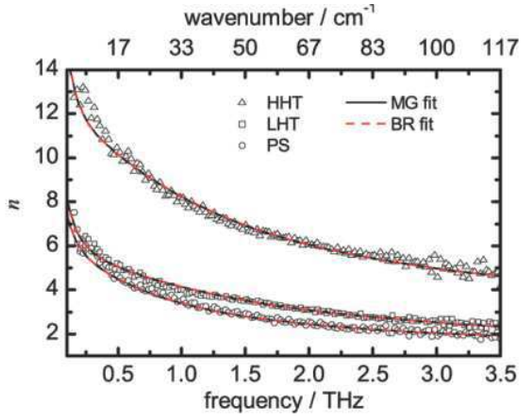

Figure 4. Real refractive index plotted for the three CNF samples. The solid and dotted lines are the real refractive indices calculated by using the Drude−Lorentz model combined with two effective medium approximation models (Maxwell−Garnett and Bruggeman).

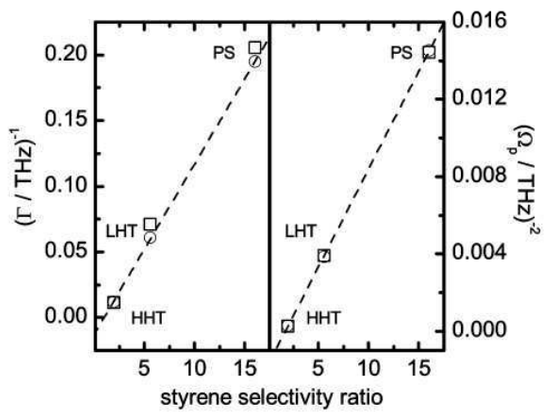

Figure 6. Correlations of Ω_p and Γ with the selectivity of styrene to other hydrocarbon products for the three CNF samples: circles, Maxwell−Garnett model parameters; squares, Bruggeman model parameters.

Motivation

Permittivity

Refractive index

Fermi level

Resistivity

Ionic conductivity

Inductance

Conductance

Permeability

Plasma frequency

Impedance

?

Semiconductor

Resistance

Ohm`s law

Schottky barrier

Drude-Lorentz model

Space charge region

Dielectric constant

Electronic conductivity

Electrochemical potential

Redox potential

Dielectric loss

Capacitance

Admittance

Basics

Basics: Interaction of materials with electromagnetic fields

- Microscopic scale (energy bands for electrons, magnetic moments of atoms and molecules)
- Macroscopic scale (overall response of macroscopic materials to external electromagnetic fields)

Macroscopic scale

Interaction between macroscopic material and electromagnetic fields generally described by **Maxwell`s equations**:

In vacuum:

$$\nabla \cdot \boldsymbol{E} = \frac{\rho}{\varepsilon_0}$$

(flux of ***E*** through a closed surface) = (charge in the interior)/ε_0 *[Gauß`law]*

$$\nabla \cdot \boldsymbol{B} = 0$$

(flux of ***B*** through a closed surface) = 0

$$\nabla \times \boldsymbol{E} = -\frac{\partial \boldsymbol{B}}{\partial t}$$

(line integral of ***E*** around a loop) =-d(flux of ***B*** through the loop)/dt *[Faraday`s law of induction]*

$$c^2 \nabla \times \boldsymbol{B} = \frac{\boldsymbol{J}}{\varepsilon_0} + \frac{\partial \boldsymbol{E}}{\partial t}$$

c^2(line integral of ***B*** around a loop) =(current through loop)/ε_0 +d(flux of ***E*** through the loop)/dt

E…electric field strength; ρ…charge density; ***B***…magnetic induction (magnetic flux density); ***J***…current density; ε_0…vacuum permittivity; c…speed of light

Macroscopic scale

In material:

$$\nabla \cdot \boldsymbol{E} = -\frac{\nabla \cdot \boldsymbol{P}}{\varepsilon_0} \text{ or } \nabla \cdot \boldsymbol{D} = \rho$$

$$\nabla \cdot \boldsymbol{B} = 0$$

$$c^2 \nabla \times \boldsymbol{B} = \frac{\partial}{\partial t}\left(\frac{\boldsymbol{P}}{\varepsilon_0} + \boldsymbol{E}\right) = \frac{1}{\varepsilon_0}\left(\boldsymbol{J} + \frac{\partial \boldsymbol{D}}{\partial t}\right) \text{ or } \nabla \times \boldsymbol{H} = \boldsymbol{J}^* + \frac{\partial \boldsymbol{D}}{\partial t}$$

$$\nabla \times \boldsymbol{E} = -\frac{\partial \boldsymbol{B}}{\partial t}$$

With the following constitutive relations:

$$\boldsymbol{D} = \varepsilon \boldsymbol{E} = (\varepsilon' - i\varepsilon'')\boldsymbol{E}$$

$$\boldsymbol{B} = \mu \boldsymbol{H} = (\mu' - i\mu'')\boldsymbol{H}$$

$$\boldsymbol{J} = \sigma \boldsymbol{E} = (\sigma' - i\sigma'')\boldsymbol{E}$$

$$\boldsymbol{P} = \alpha \boldsymbol{E}$$

*Material is described by **permittivity** (electric field, bound and free electrons), **permeability** (magnetic field, unpaired electrons), and **conductivity** (electric field, free electrons)*

P…Polarization; α…Polarizability; ***D***…electric displacement; ***H***…magnetic field strength; $\varepsilon = \varepsilon' - i\varepsilon''$…complex permittivity of the material; $\mu = \mu' - i\mu''$…complex permeability of the material; $\sigma = \sigma' - i\sigma''$…complex conductivity of the material

1st case: Low-conductivity materials

Conductivity σ is small → electromagnetic properties defined by permittivity ε (response to electric fields) and permeability μ (response to magnetic fields)

In vacuum:

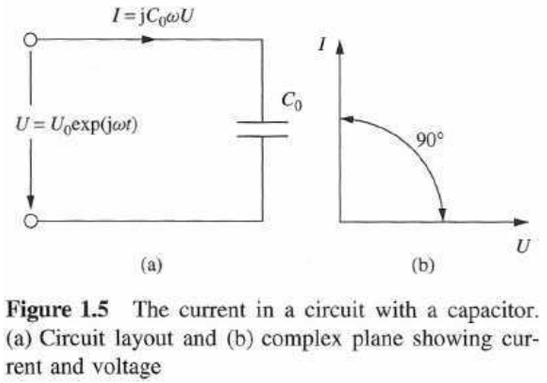

Figure 1.5 The current in a circuit with a capacitor. (a) Circuit layout and (b) complex plane showing current and voltage

$$I = \frac{dQ}{dt} = \frac{d}{dt}(C_0 U_0 e^{i\omega t}) = iC_0\omega U$$

Current leads the voltage by a phase angle of 90°

I…current; Q…charge; C_0…capacitance; U…ac voltage

After insertion of a dielectric material into the capacitor:

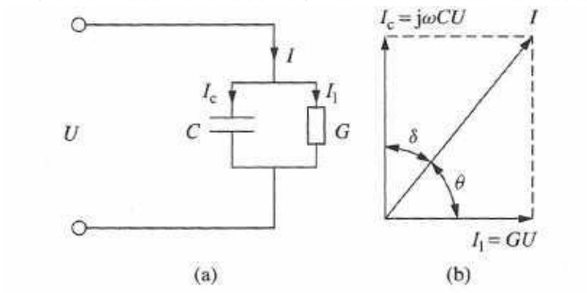

Figure 1.6 The relationships between charging current and loss current. (a) Equivalent circuit and (b) complex plane showing charging current and loss current

L. F: Chen et al., *Microwave Electronics,* J. Wiley & Sons **2004**

$$I = I_c + I_l = iC\omega U + GU = (iC\omega + G)U$$

I_c leads I_l by 90°, I leads U with less than 90°; phase angle between I_c and I = *loss angle* δ

I…total current; I_c…charging current; I_l…loss current;
C…capacitance of the capicitor with dielectric material;
G…conductance of dielectric material

Basics: Interaction of materials with electromagnetic fields

Capacitance after insertion of dielectric material:

$$C = \frac{\varepsilon C_0}{\varepsilon_0} = (\varepsilon' - \mathrm{i}\varepsilon'')\frac{C_0}{\varepsilon_0}$$

Charging current:

$$I_c = (\mathrm{i}\omega\varepsilon' + \omega\varepsilon'')\frac{C_0}{\varepsilon_0}U$$

Current density ***J*** transverse to capacitor under applied field strength ***E***:

$$J = (\mathrm{i}\omega\varepsilon' + \omega\varepsilon'')E = \varepsilon\frac{\mathrm{d}E}{\mathrm{d}t}$$

energy storage (bound electrons)

$= \sigma$(dielectric conductivity)

energy loss (free and bound electrons)

Energy dissipation described by dielectric loss tangent:

$$\tan\delta_e = \frac{\varepsilon''}{\varepsilon'}$$

Or by the quality factor:

$$Q_e = \frac{\varepsilon'}{\varepsilon''} = \frac{1}{\tan\delta_e}$$

Usually dimensionless relative permittivities are used:

$$\varepsilon_r = \frac{\varepsilon}{\varepsilon_0} = \frac{\varepsilon' - \mathrm{i}\varepsilon''}{\varepsilon_0} = \varepsilon_r' - \mathrm{i}\varepsilon_r''$$

Debye equation

Debye equation: $\varepsilon(\omega) = \varepsilon_\infty + \frac{\varepsilon_s - \varepsilon_\infty}{1 + j\omega\tau}$

For $\omega = 0,\ \varepsilon(0) = \varepsilon_s$

For $\omega = \infty,\ \varepsilon(\infty) = \varepsilon_\infty$

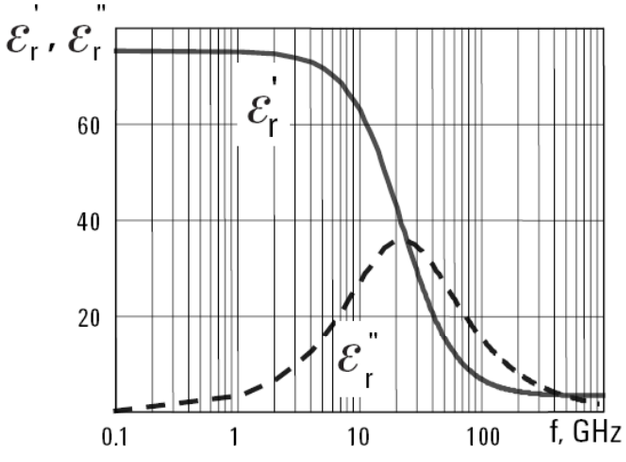

$$\tan\delta = \frac{\varepsilon''_r}{\varepsilon'_r} = D = \frac{1}{Q} = \frac{\text{Energy Lost per Cycle}}{\text{Energy Stored per Cycle}}$$

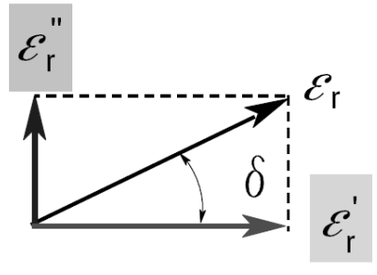

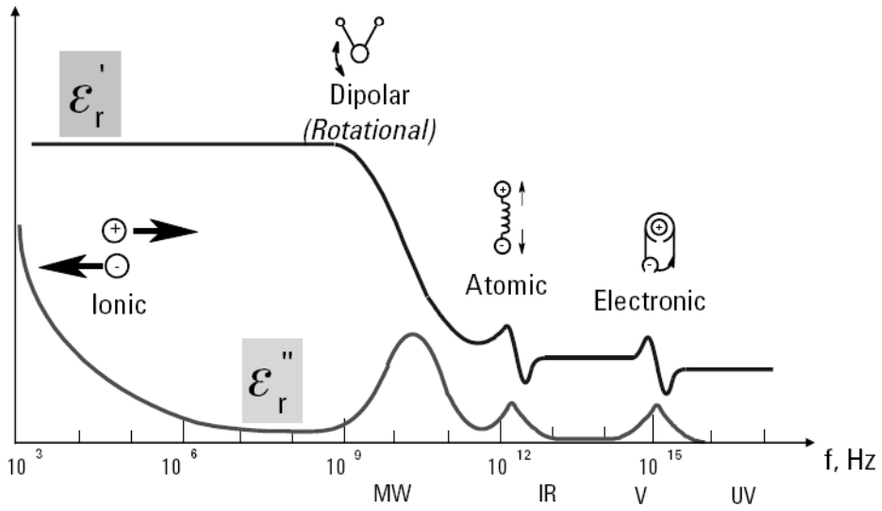

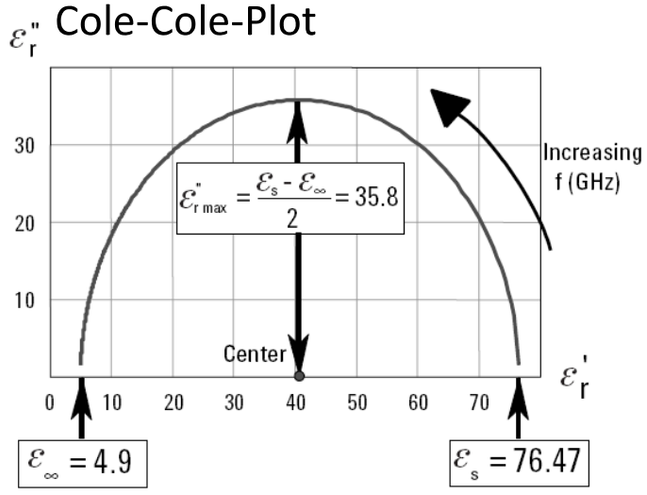

Basics of Measuring the Dielectric Properties of Materials, *Agilent Application Note* **2006**

Electromagnetic waves in a dielectric medium

Determined by characteristic wave impedance η of the medium *(intrinsic impedance)* and wave velocity v in the medium

Characteristic impedance η = total electric field/total magnetic field in a plane perpendicular to the propagation direction:

$$\eta = \sqrt{\frac{\mu}{\varepsilon}}$$

$$v = \frac{1}{\sqrt{\mu\varepsilon}}$$

Complex propagation coefficient γ:

$$\gamma = \alpha + \mathrm{i}\beta = \mathrm{i}\underbrace{\omega\sqrt{\mu\varepsilon}}_{\text{wave vector } \boldsymbol{k}} = \mathrm{i}\frac{\omega}{\mathrm{c}}\sqrt{\mu_r\varepsilon_r} = \mathrm{i}\frac{\omega}{\mathrm{c}}n$$

α…attenuation coefficient; β=2π/λ…phase change coefficient; λ…operating wavelength; n…complex index of refraction

Basics: Interaction of materials with electromagnetic fields

- E.g.: wave propagating in z-direction, polarized in x-direction:

$E_x = E_0 \exp[i(\omega t - kz)]$

$n = kc/\omega = n' - in''$

$E_x = E_0 \exp[i\omega(t - nz/c)] = E_0 \exp(-\omega n'' z/c) \cdot \exp[i\omega(t - n' z/c)]$

Amplitude decays exponentially with z
→ Energy loss/absorption by atomic oscillators

Wave propagating with c/n'
→ "normal" index of refraction

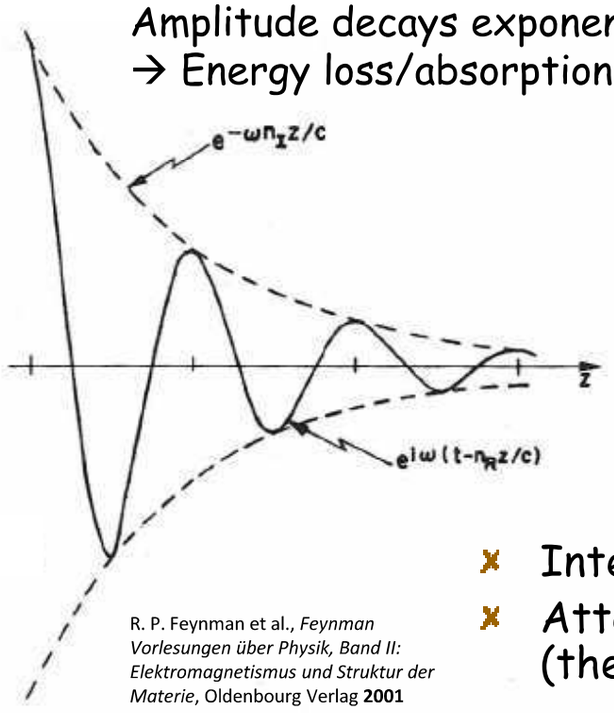

R. P. Feynman et al., *Feynman Vorlesungen über Physik, Band II: Elektromagnetismus und Struktur der Materie*, Oldenbourg Verlag **2001**

- Intensity ~ Amplitude^2 = $\exp[-2\omega n'' z/c] = \exp(-\alpha z)$
- Attenuation/absorption coefficient $\alpha = 2\omega c n''/c$ (theory of light absorption)

2nd case: High-conductivity materials (metals)

Effects of bound electrons very small (can be described like before), properties dominated by free conduction electrons

Definition of conductivity: $\boldsymbol{J} = \sigma \boldsymbol{E} = (\sigma' + \mathrm{i}\sigma'')\boldsymbol{E}$ **(Ohm´s law)**

Index of refraction of metals for rather low frequencies ($\omega \ll \sigma/\varepsilon_0$): $n = \sqrt{\frac{\sigma}{2\varepsilon_0 \omega}}(1-\mathrm{i})$

Amplitude of wave in z direction:

$$\exp\left[-\sqrt{\frac{\sigma\omega}{2\varepsilon_0 c^2}}z\right] = \exp\left[-\frac{z}{\delta}\right]$$

Skin depth δ: $\delta = \sqrt{\frac{2\varepsilon_0 c^2}{\sigma\omega}}$

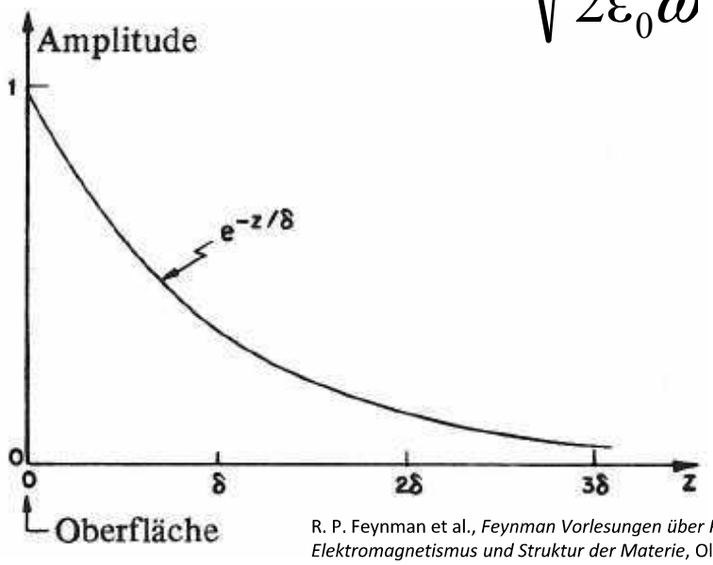

R. P. Feynman et al., *Feynman Vorlesungen über Physik, Band II: Elektromagnetismus und Struktur der Materie*, Oldenbourg Verlag **2001**

Basics: Interaction of materials with electromagnetic fields

Skin depth: $\delta = \sqrt{\frac{2\varepsilon_0 c^2}{\sigma\omega}}$

Ag: σ= 61.39x10^6 Sm^{-1}
→$\delta(\nu$ = 9 GHz) = 6.77x10^{-7} m = 677 nm
→$\delta(\nu$ = 100 GHz) = 2.03x10^{-7} m = 203 nm

VPO: $\sigma \approx 10^{-3}$ Sm^{-1}
→$\delta(\nu$ = 9 GHz) = 0.17 m
→$\delta(\nu$ = 100 GHz) = 0.05 m

RuO_2: σ= 2x10^6 Sm^{-1} (300 K)
→$\delta(\nu$ = 9 GHz) = 3.8 µm
→$\delta(\nu$ = 100 GHz) = 1.1 µm

Basics: Interaction of materials with electromagnetic fields

Metals at high frequencies:

$$n^2 = 1 - \frac{\sigma}{\varepsilon_0 \omega^2 \tau} = 1 - \underbrace{\frac{N q_e^2}{m_e \varepsilon_0}} \frac{1}{\omega^2}$$

(Drude (Lorentz) model of electrical conduction)

Drude plasma frequency^2: ω_p^2

$$\boldsymbol{J} = \sigma \boldsymbol{E} = \frac{N q_e^2 \tau}{m_e} \boldsymbol{E}$$

Wikipedia: The model, which is an application of kinetic theory, assumes that the microscopic behavior of electrons in a solid may be treated classically and looks much like a table football machine, with a sea of constantly jittering electrons bouncing and re-bouncing off heavier, relatively immobile positive ions.

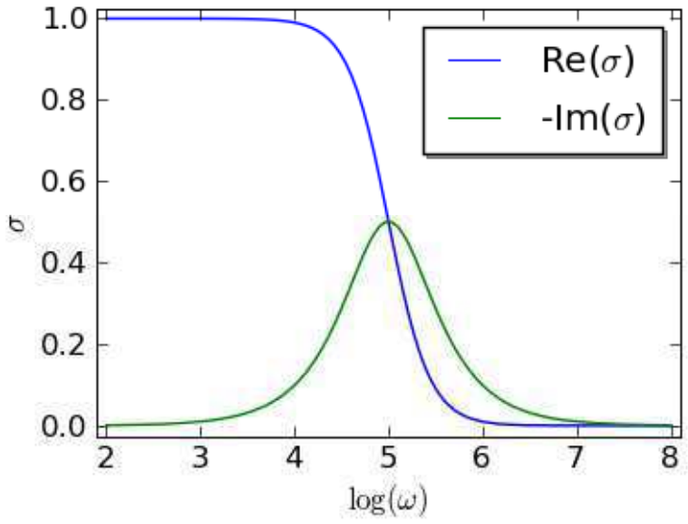

$\omega < \omega_p$: Imaginary part of n or σ exists → attenuation of waves
$\omega >> \omega_p$: Index is real → metal becomes transparent

τ…mean free time between electron collisions; N…electron density; q_e…electron charge; m_e…electron mass

Microscopic scale

Electron energy bands

Insulators

Semiconductors

Conductors

Magnetic moments

Diamagnetic

Paramagnetic

Ordered magnetic materials

Basics: Interaction of materials with electromagnetic fields

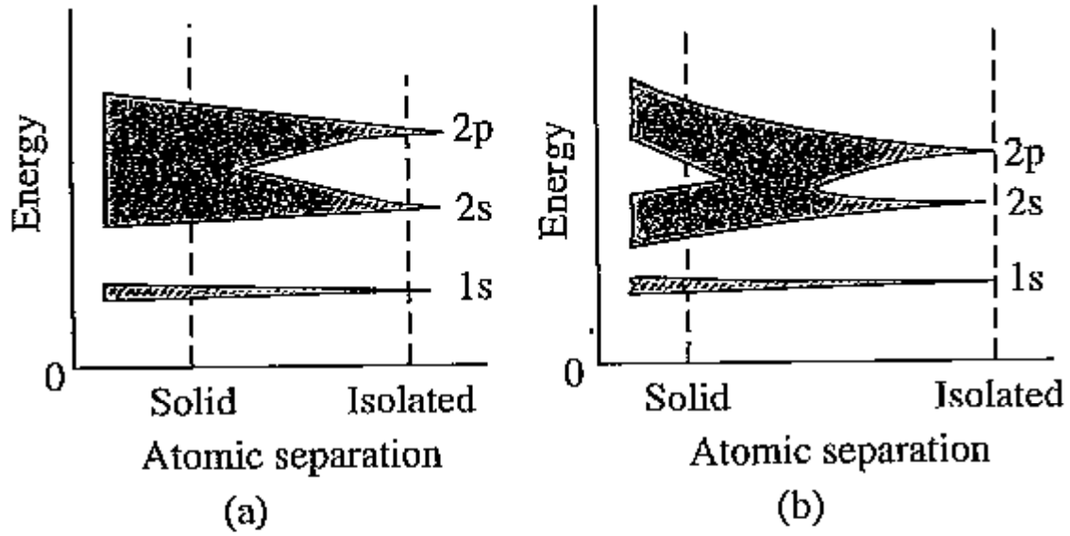

Figure 1.1 The relationships between energy bands and atomic separation. (a) Energy bands of lithium and (b) energy bands of carbon. (Bolton 1992) Source: Bolton, W. (1992), *Electrical and Magnetic Properties of Materials*, Longman Scientific & Technical, Harlow

L. F: Chen et al., *Microwave Electronics,* J. Wiley & Sons **2004**

Basics: Interaction of materials with electromagnetic fields

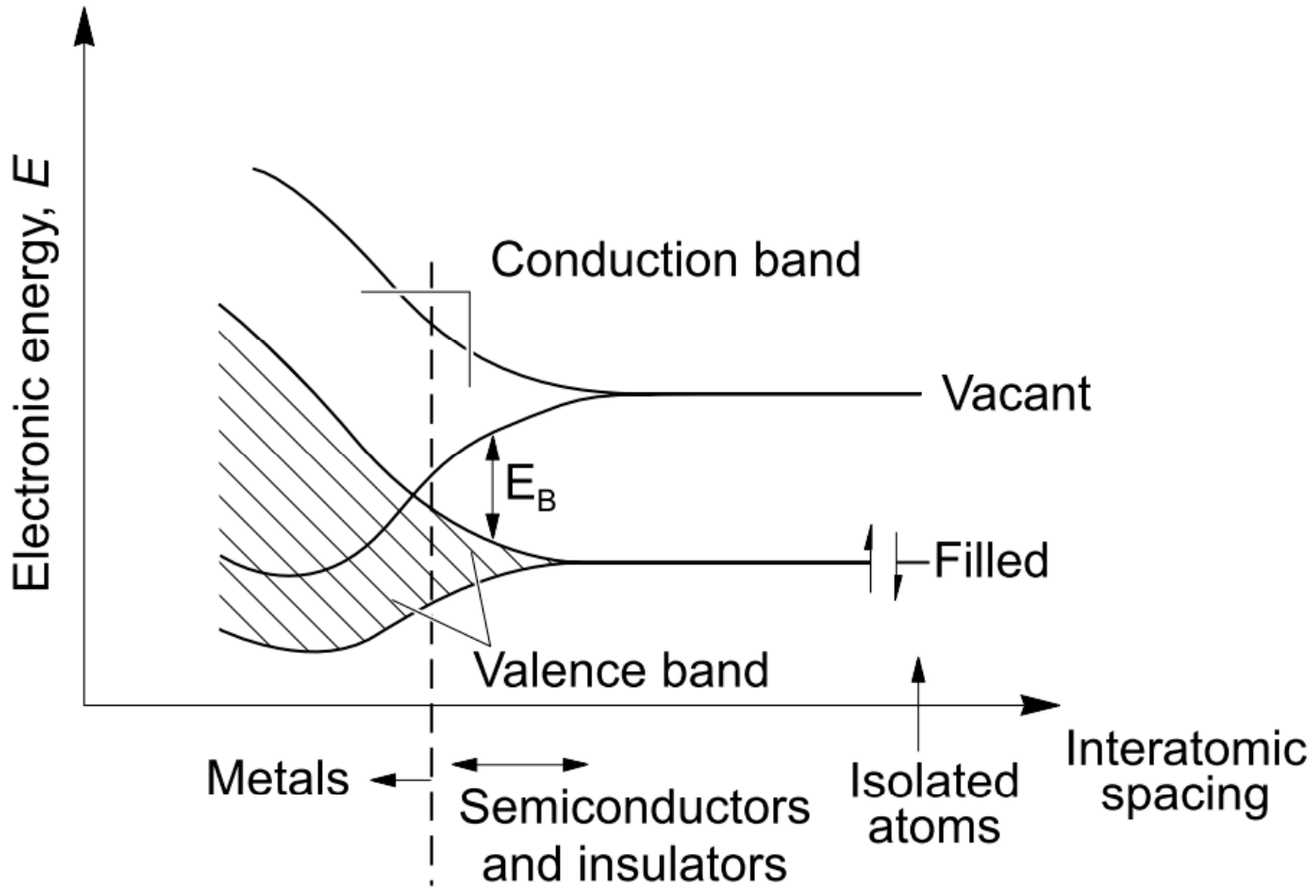

A. W. Bott, *Current Separations* **1998**, *17*, 87

Occupancy of electrons in a band is determined by **Fermi-Dirac statistics**

Fermi-Dirac distribution (for an electron gas):

$$f(E) = \frac{1}{\exp\left(\frac{E-\mu}{k_B T}\right)+1}$$

E...Energy

k_B...Boltzmann constant

T...Temperature

μ...(Electro-)Chemical potential

$$\mu(T=0) = E_{Fermi}$$

$$f(E=\mu) = 1/2$$

= Fermi level

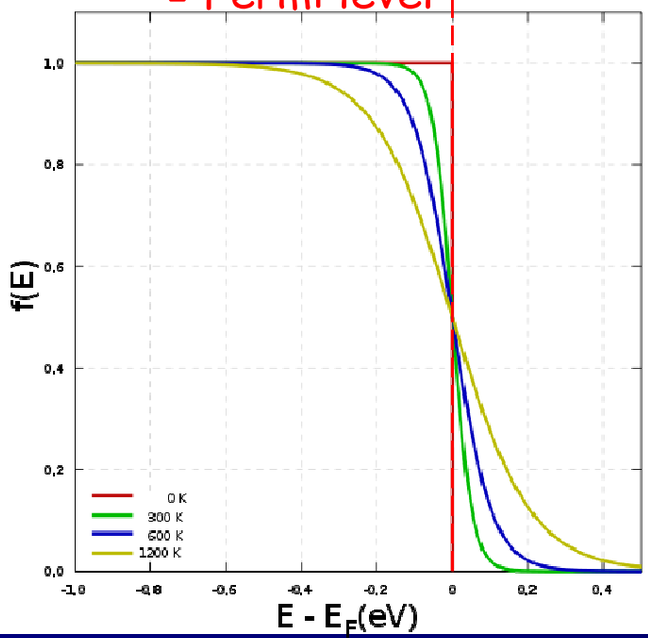

P. A. Tipler, *Physik*, Spektrum Verlag

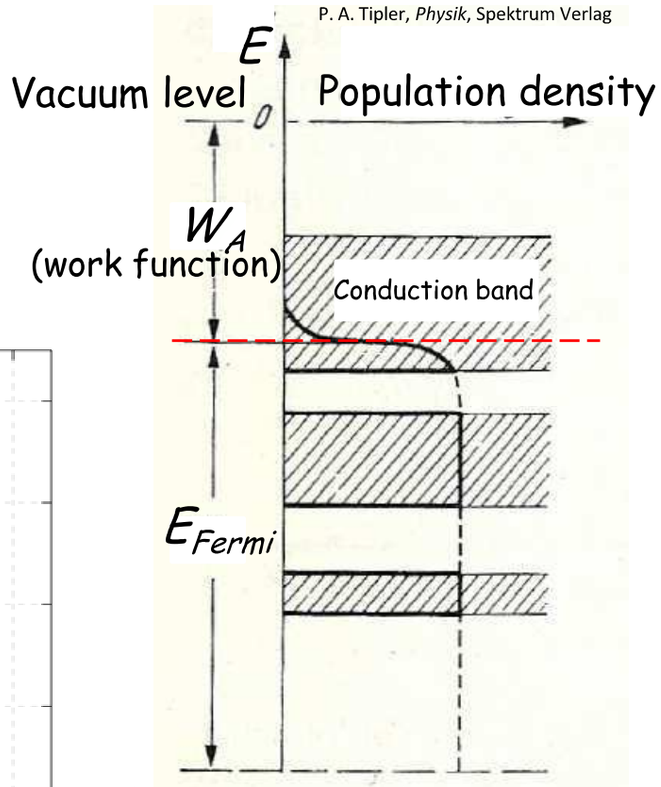

The Fermi curve determines the population of occupied states, independent of the existence of states in the regarded E region

Basics: Interaction of materials with electromagnetic fields

Intrinsic semiconductor

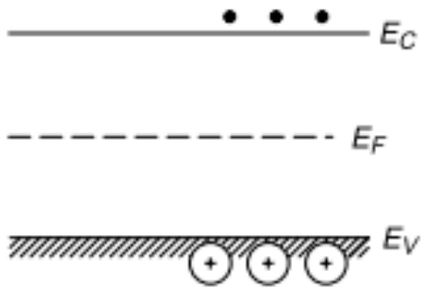

e.g. Si (band gap at 300 K = 1.12 eV)

(Extrinsic) n-type semiconductor

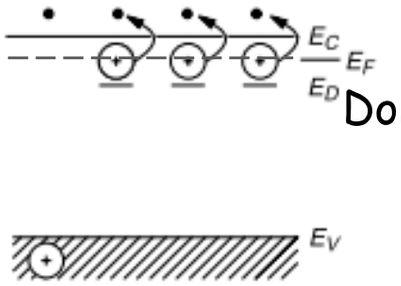

e.g. As-doped Si

additional electrons

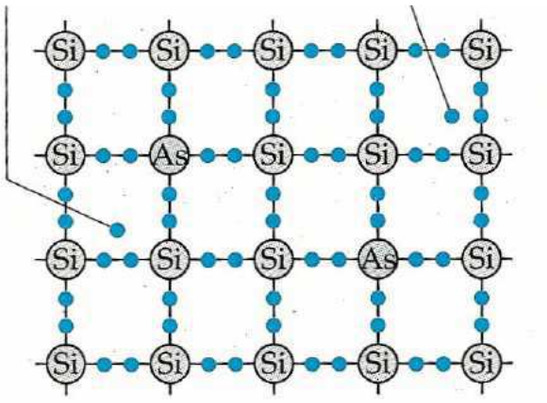

(Extrinsic) p-type semiconductor

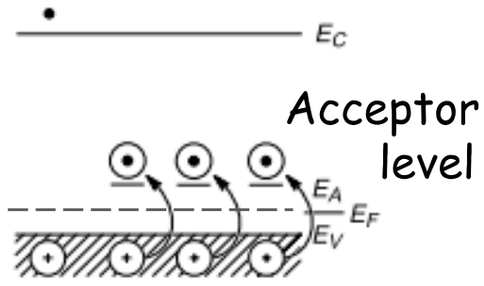

e.g. Ga-doped Si

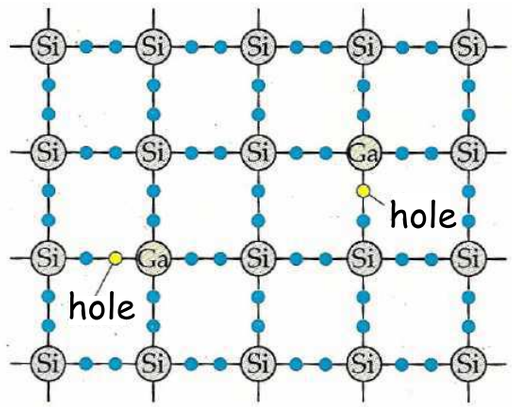

P. A. Tipler, *Physik*, Spektrum Verlag

Space charge region

Space charge region

Metals

Contact voltage = $(W_{A1} - W_{A2})/e$

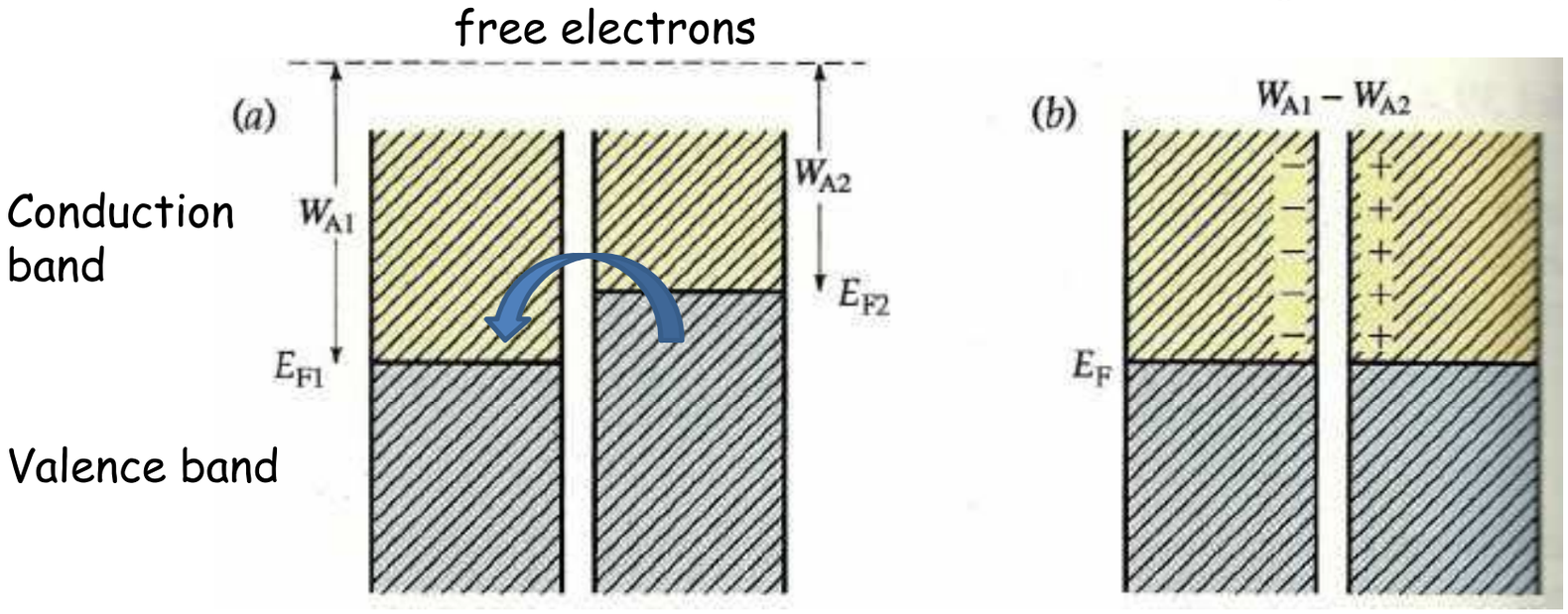

a) Energy states of two different metals with different Fermi energies and work functions. b) With contact, electrons will flow from the metal with higher Fermi energy (lower work function) to the one with lower Fermi energy (larger work function) until the Fermi levels of both metals are equalized

P. A. Tipler, *Physik*, Spektrum Verlag

Space charge region

Semiconductors

n-type SC in contact with electrolyte

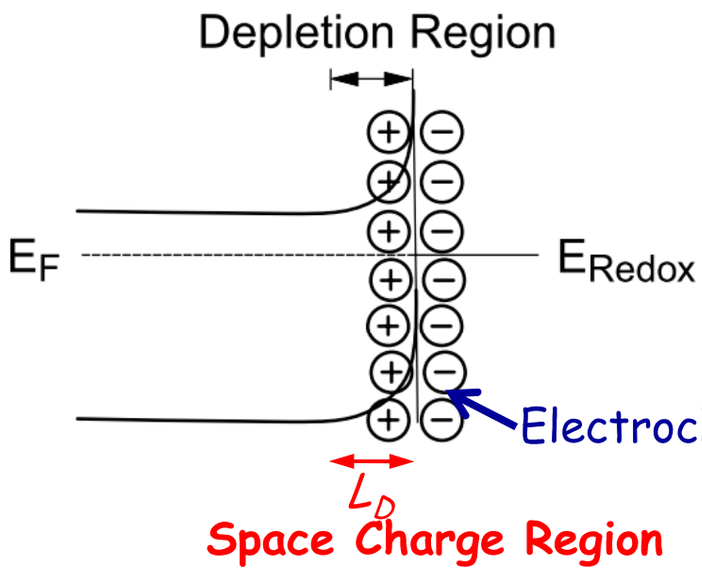

p-type SC in contact with electrolyte

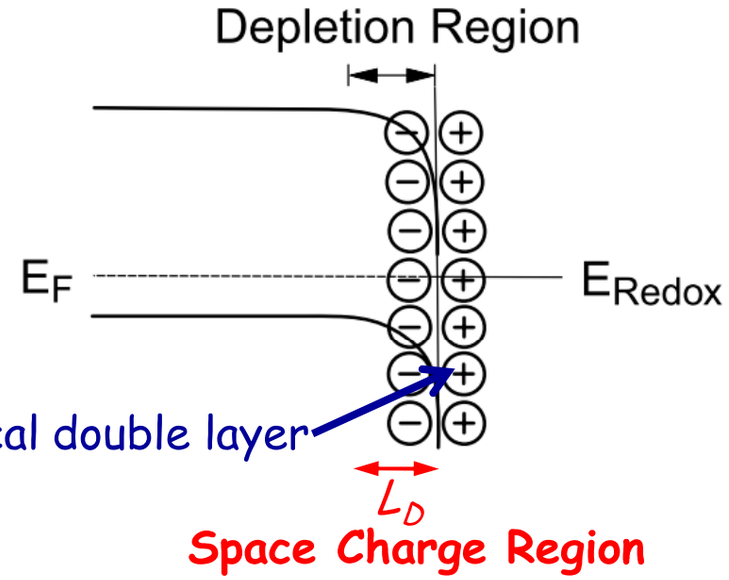

In metals: penetration depth (space charge region to compensate surface charge) of only a few lattice constants (high concentration of free charge carriers)

In SCs: Debye shielding, L_D, can amount from 10 nm to 1 μm

$$L_D = \sqrt{\frac{\varepsilon k_B T}{2\pi q^2 n_i}}$$

ε...Dielectric permittivity of crystal; q...Electron charge; n_i...Concentration of charge carriers in intrinsic semiconductor

A. W. Bott, *Current Separations* **1998**, *17*, 87

Space charge region

External Potential Control

Effect of varying the applied potential (E) on the band edges in the interior of an n-type semiconductor.
a) $E > E_{fb}$, b) $E = E_{fb}$, c) $E < E_{fb}$.

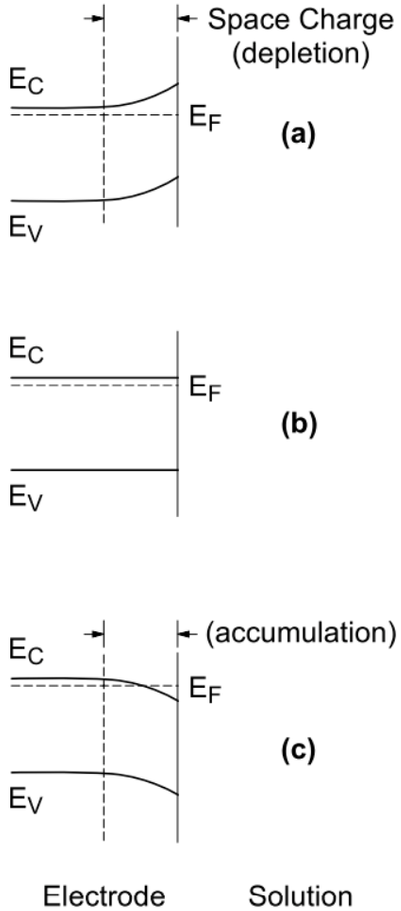

Positive potential

Flatband potential

Negative potential

Effect of varying the applied potential (E) on the band edges in the interior of a p-type semiconductor.
a) $E > E_{fb}$, b) $E = E_{fb}$, c) $E < E_{fb}$.

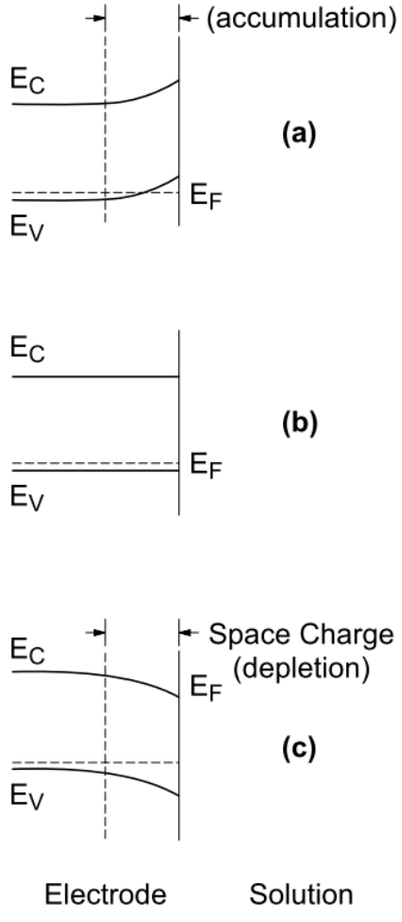

A. W. Bott, *Current Separations* **1998**, *17*, 87

Space charge region

p-n junction

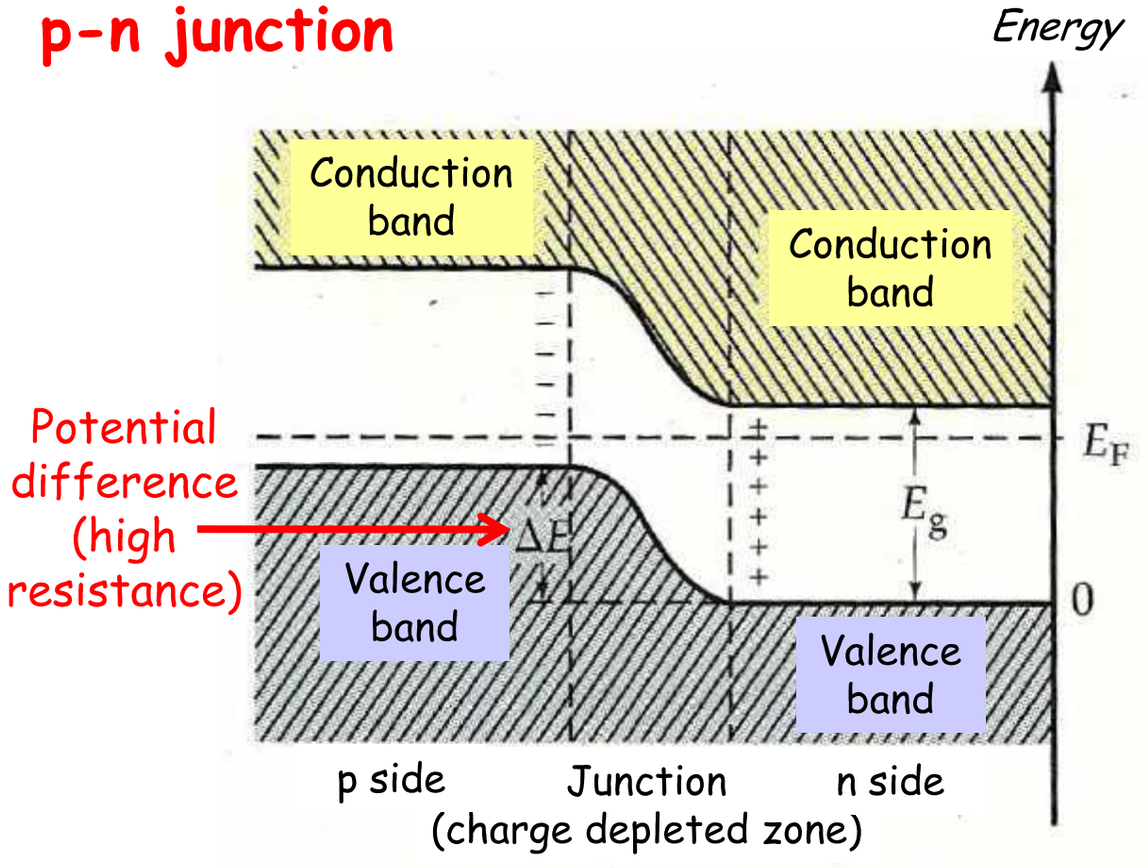

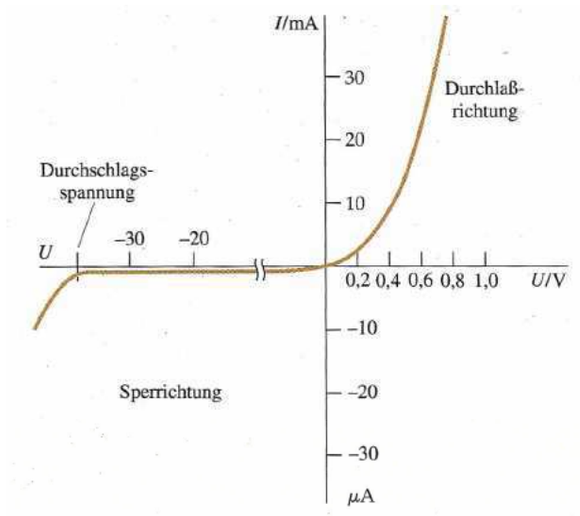

Electrons migrate to p side, holes migrate to n side until electrochemical potentials (Fermi energies) are equilibrated

P. A. Tipler, *Physik*, Spektrum Verlag

Metal-semiconductor junction (Schottky barrier)

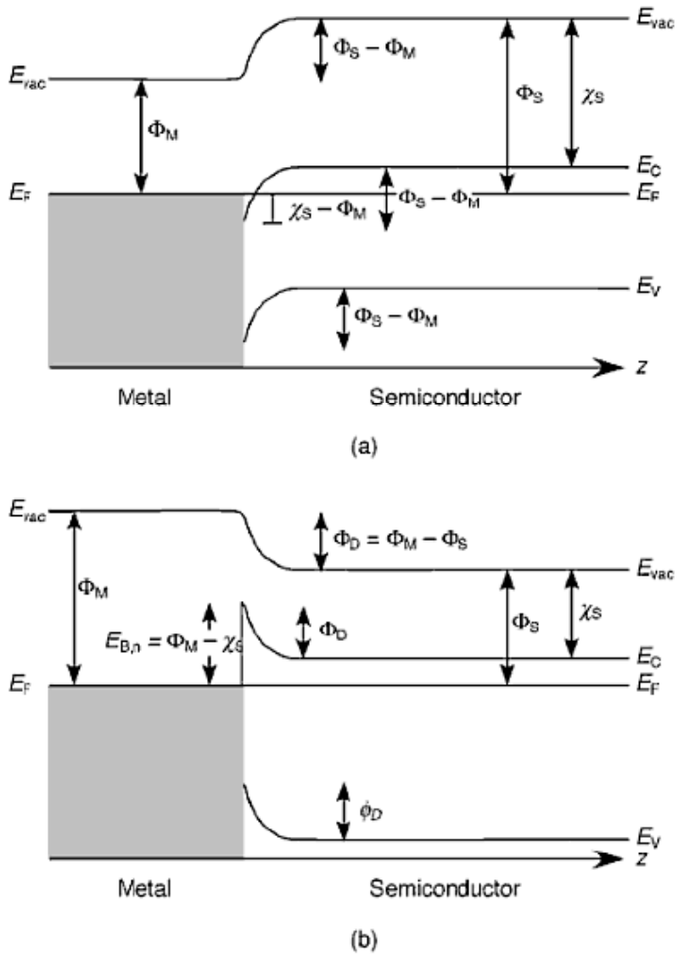

Ohmic contact

Schottky barrier

Figure 1.17 *Band bending in an n-type semiconductor at a heterojunction with a metal. (a) Ohmic contact ($\Phi_S > \Phi_M$). (b) Blocking contact (Schottky barrier, $\Phi_S < \Phi_M$). The energy of the bands is plotted as a function of distance z in a direction normal to the surface. Φ_S, Φ_M work function of the semiconductor and of the metal, respectively; E_{vac}, vacuum energy; E_C, energy of the conduction band minimum; E_F, Fermi energy; E_V energy of the valence band maximum. Redrawn from S. Elliott, The Physics and Chemistry of Solids. (1998) Copyright, with permission from John Wiley & Sons, Ltd.*

K. W. Kolasinski, *Surface Science: Foundations of Catalysis and Nanoscience*, John Wiley & Sons **2008**

Space charge region

External Potential Control

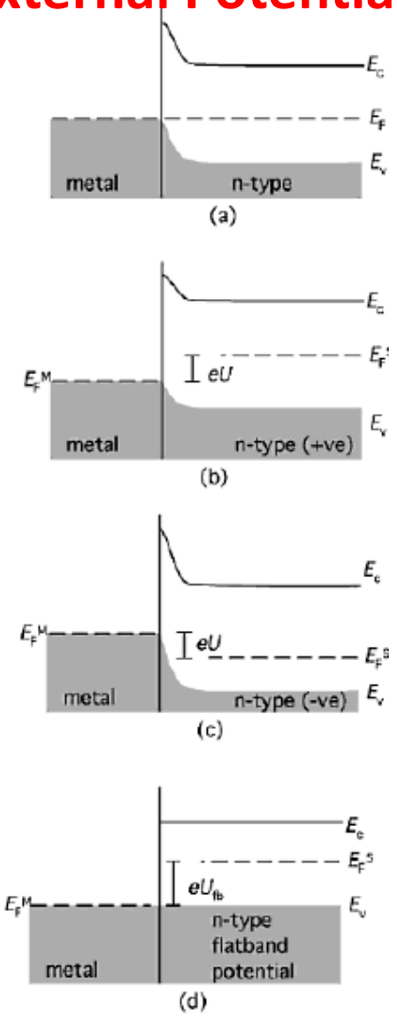

No bias

Forward bias

Figure 1.18 *The electrochemical potential and the effects of an applied voltage on a metal–semiconductor interface. (a) No applied bias. (b) Forward bias. (c) Reverse bias. (d) Biased at the flatband potential, U_{fb}. E_C, energy of the conduction band minimum; E_F, Fermi energy; E_V, energy of the valence band maximum; superscripts M and S refer to the metal and the semiconductor, respectively.*

Reversed bias

Biased at flatband potential

K. W. Kolasinski, *Surface Science: Foundations of Catalysis and Nanoscience*, John Wiley & Sons **2008**

Adsorption and Catalysis

Adsorption → Catalysis

= Schottky barrier height

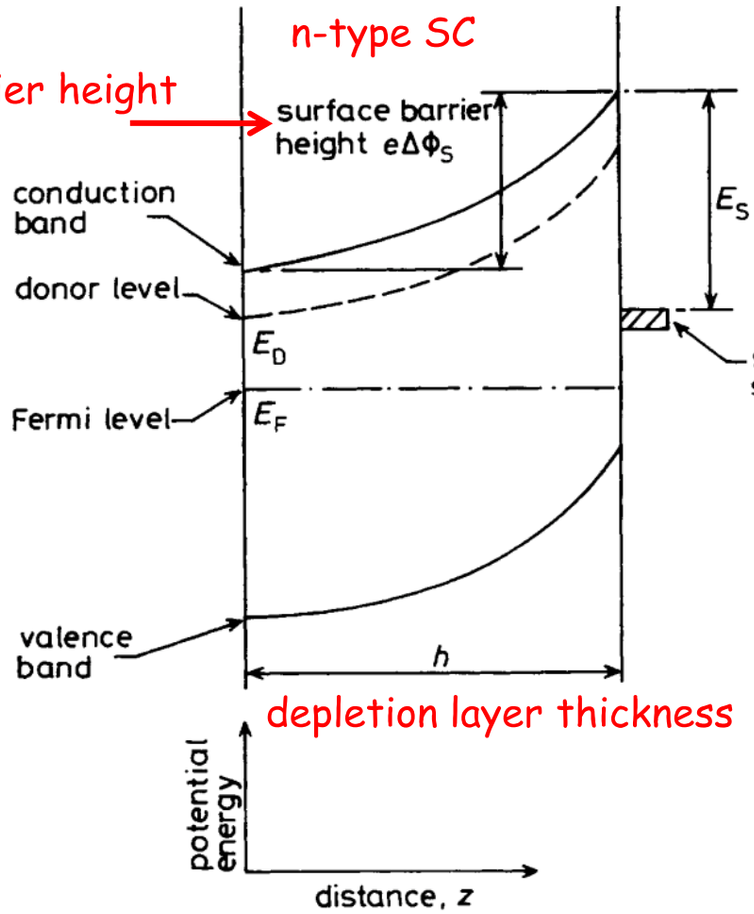

$$n' + \tfrac{1}{2}O_2(g) \overset{k_1}{\rightleftharpoons} O_S^-$$

$$R(g) + O_S^- \overset{k_2}{\rightarrow} RO(g) + n'$$

$$\tfrac{1}{2}O_2 \rightleftharpoons O_S \rightleftharpoons O_2^- \rightleftharpoons O^- \rightleftharpoons O^{2-}$$

(O^- ⇅ $2OH^-$ via $H_2O + e^-$; O^- → RO via $R - e^-$)

J. F. McAleer et al., *J. Chem. Soc. Faraday Trans. 1* **1987**, *83*, 1323-1346

Accumulation layers
(concentration of majority charge carriers larger than in bulk)

Depletion layers
(concentration of majority charge carriers lower than in bulk)

Inversion layers
(conductivity in SCR opposite in type to that of bulk)

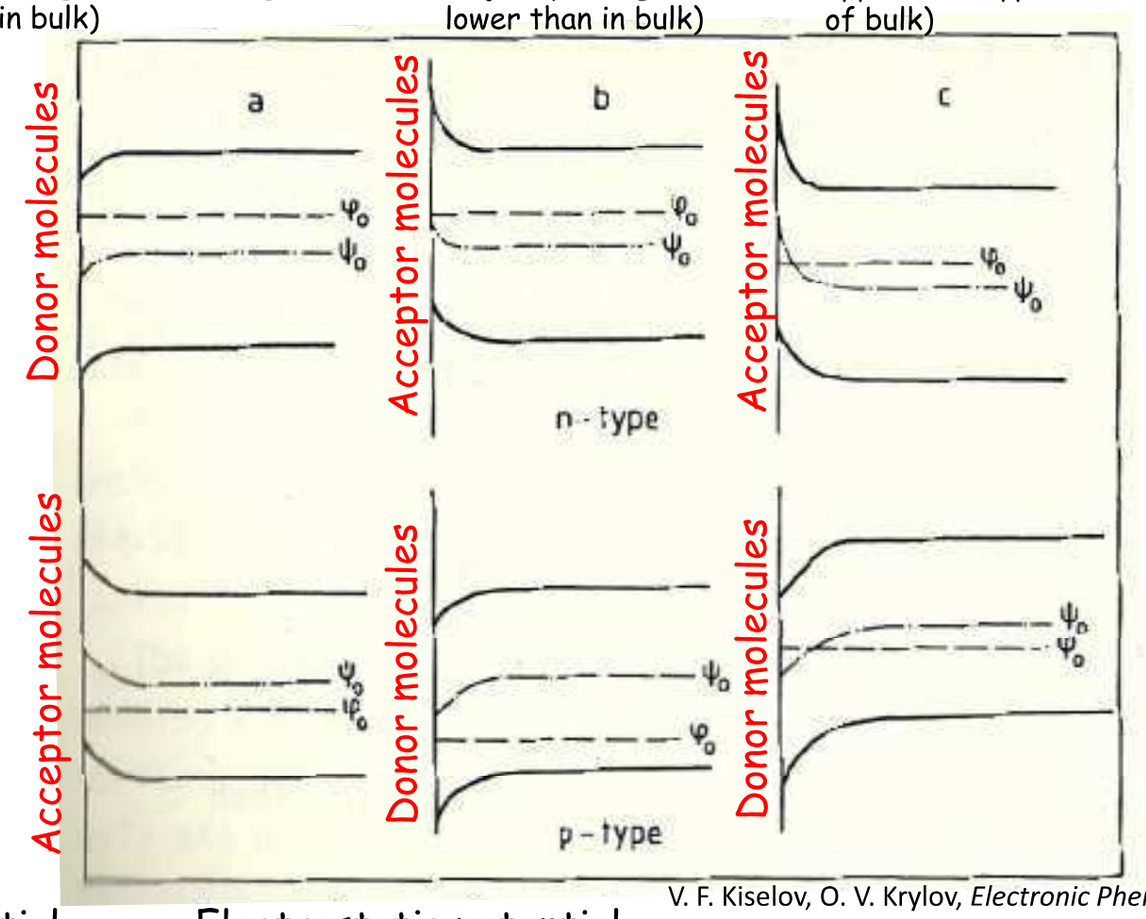

φ_0 …Fermi potential ψ_0 …Electrostatic potential

V. F. Kiselov, O. V. Krylov, *Electronic Phenomena in Adsorption and Catalysis* , Springer-Verlag **1987**

Adsorption of Donor Molecules

Water on reduced rutile

Water on oxidized and hydrated rutile

Ammonia on oxidized and hydrated rutile

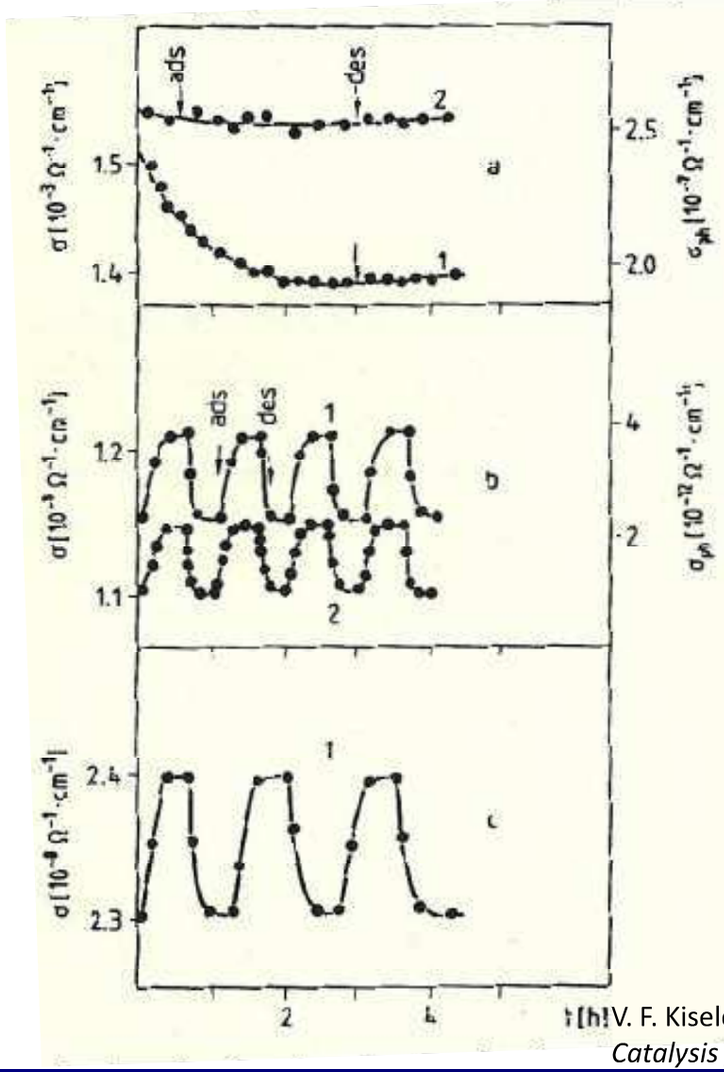

1 conductivity
2 photoconductivity

→ formation of strong coordinative bonds

Fig.6.3a-c. Variations in conductivity σ (1) and photoconductivity $\Delta\sigma_{ph}$ (2) of rutile monocrystal in adsorption-desorption cycling of water (a,b) and ammonia (c) on oxidized and hydrated (b,c) and reduced (a) specimens. First admission at t =0

V. F. Kiselov, O. V. Krylov, *Electronic Phenomena in Adsorption and Catalysis* , Springer-Verlag **1987**

Adsorption of Acceptor Molecules

Chemisorption of NO_2 on PbS

biographic states = additional set of electron surface states in the forbidden band due to domains, steps, dislocation exits, vacancies, and other defects

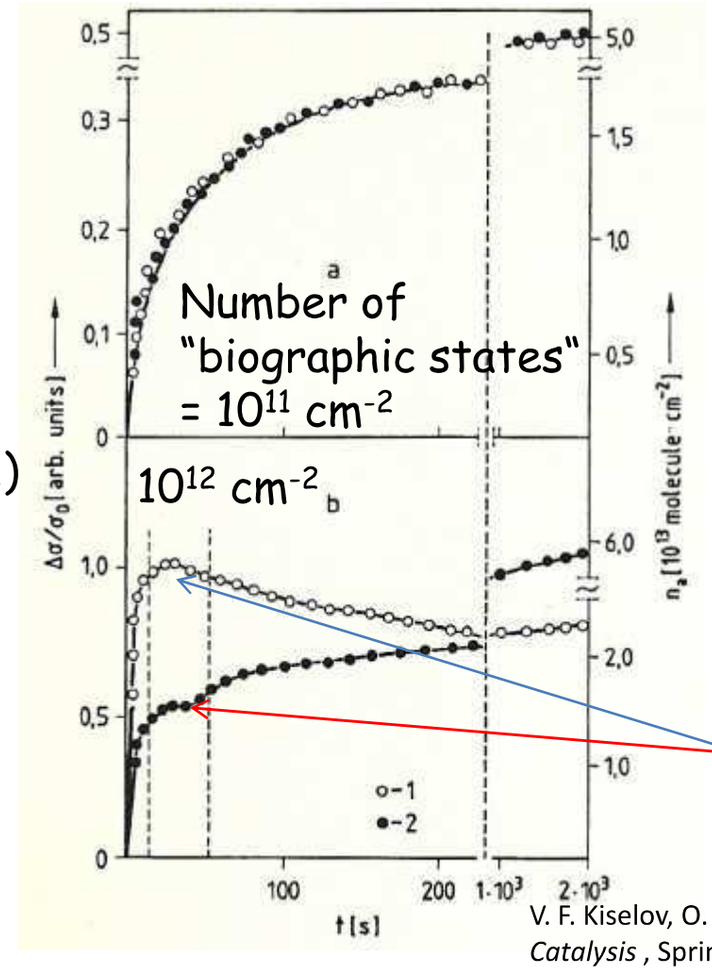

Variation in conductivity (1)

Number of chemisorbed NO_2 at p = 0.7 torr (2)

Rate of adsorption changes when the sign of $\partial Q_{ss}(t)/\partial t$ is reversed owing to recharging of a number of traps

V. F. Kiselov, O. V. Krylov, *Electronic Phenomena in Adsorption and Catalysis* , Springer-Verlag **1987**

Previous slides: Behavior of thin layers

Next slides: Behavior of massive porous bodys (real catalysts) → conductance limited by intergrain constrictions

1st scenario: well sintered case with a fully open "neck"

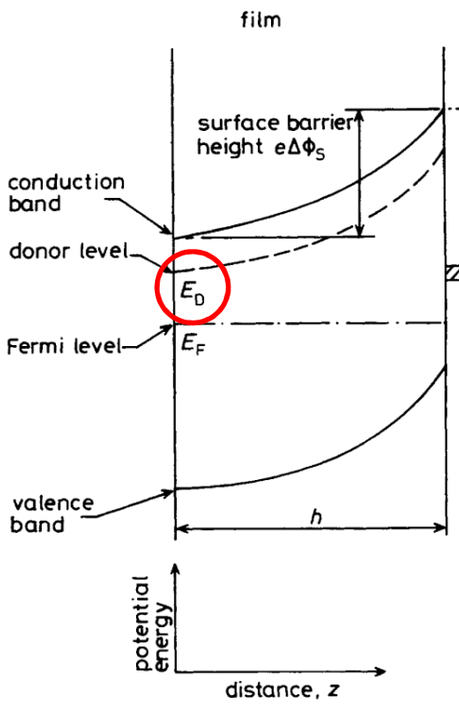

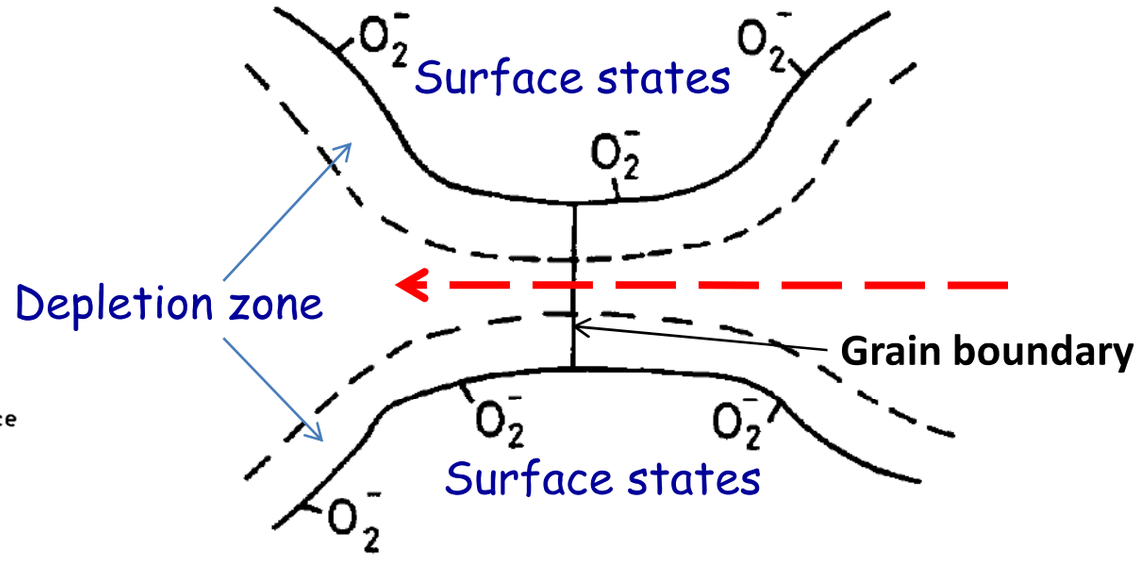

Conductivity dominated by undepleted layer in the center of the neck (lowest resistivity)
→determined by activation of electrons/holes in the bulk (bulk-trap limited regime), activation energy E_D
→ little effect of gaseous atmosphere (only on the effective channel width)

J. F. McAleer et al., *J. Chem. Soc. Faraday Trans. 1* **1987**, *83*, 1323-1346

2nd scenario: closed "neck"

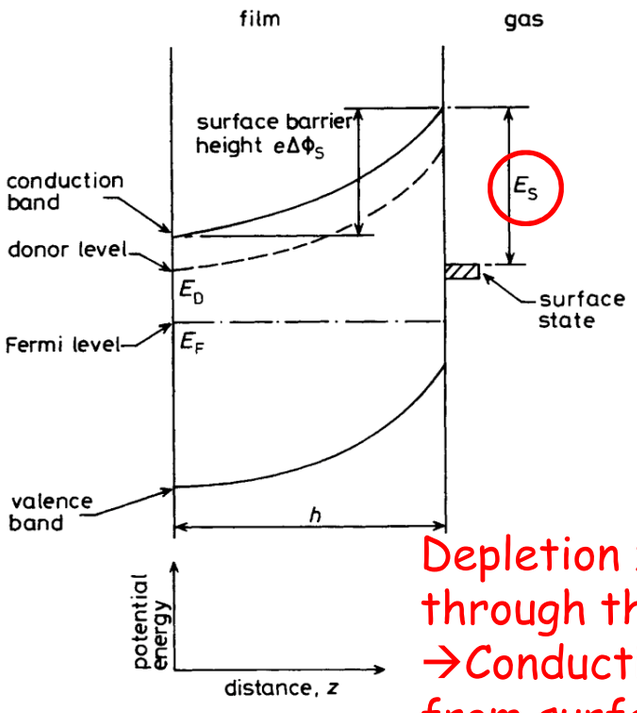

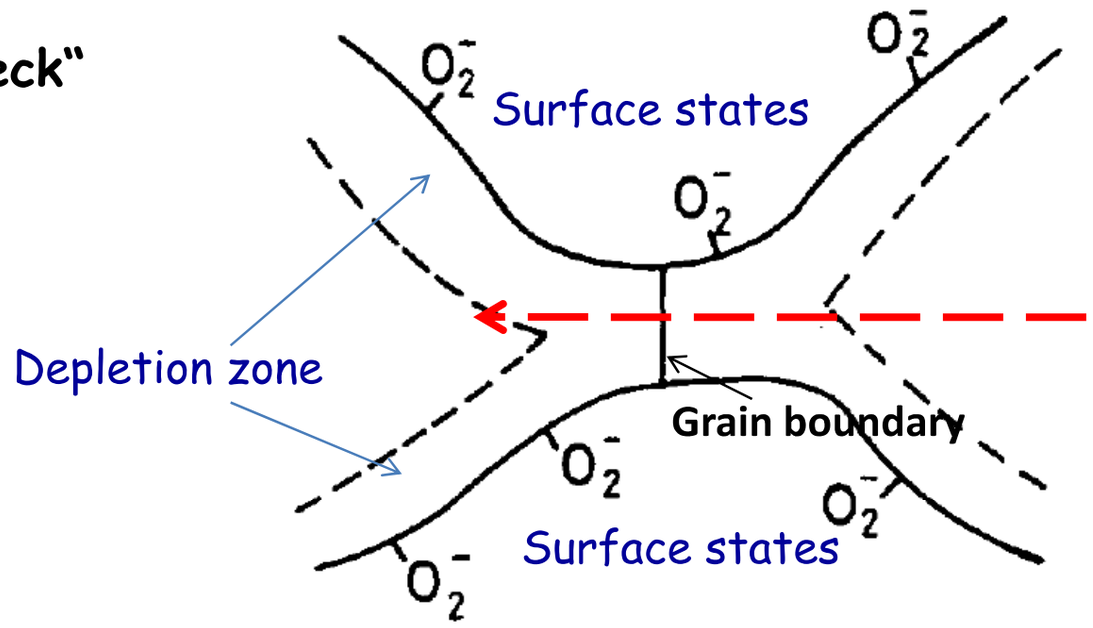

Depletion zones overlap leaving a higher resistance ohmic path through the center

→Conductivity determined by activation of electrons/holes from surface states (surface-trap limited regime), activation energy E_s

→ directly affected by influence of gas atmosphere on the occupancy of surface states

J. F. McAleer et al., *J. Chem. Soc. Faraday Trans. 1* **1987**, *83*, 1323-1346

3rd scenario: Schottky barrier

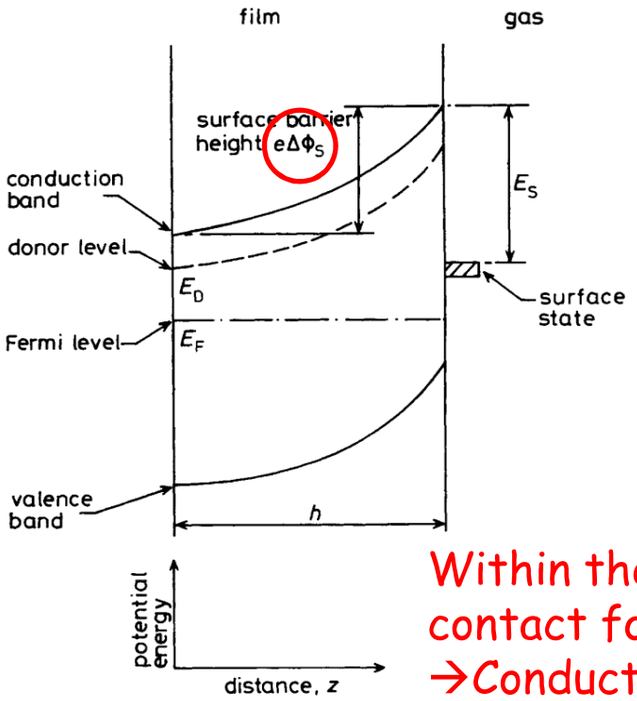

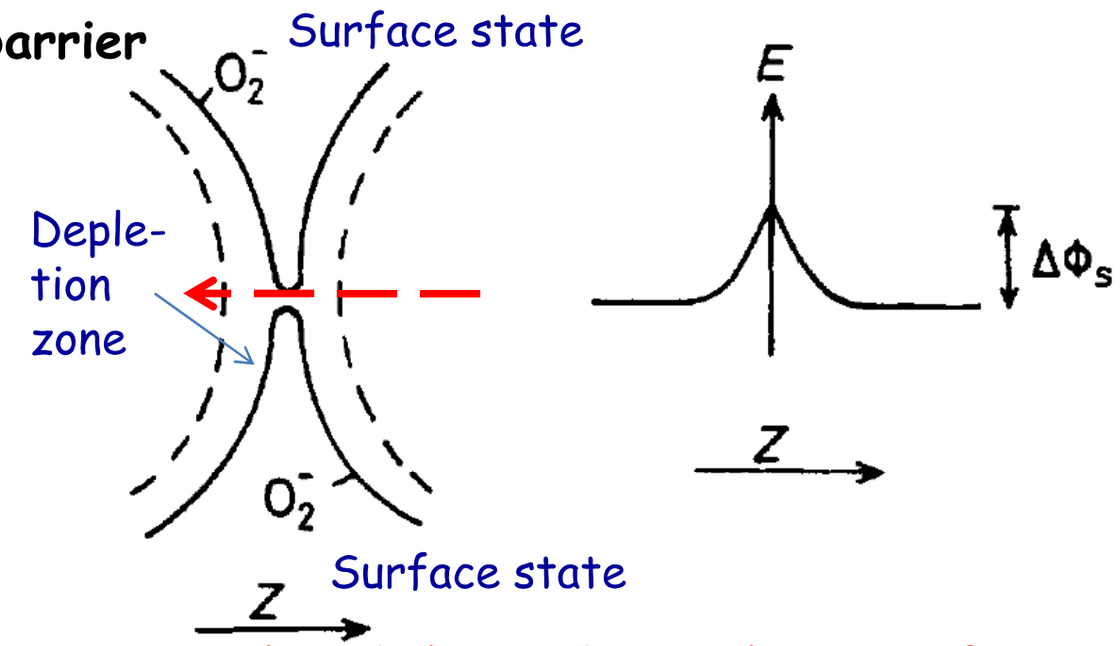

Within the two grains ohmic behavior, but at the point of contact formation of a Schottky barrier
→Conductivity limited by charge transport across the barrier;
$\sigma \approx$ constant x $\exp(-e\Delta\phi_s)/k_BT$
→ direct affected by charge and fractional coverage of surface species and hence the compostion of gas atmosphere

J. F. McAleer et al., *J. Chem. Soc. Faraday Trans. 1* **1987**, *83*, 1323-1346

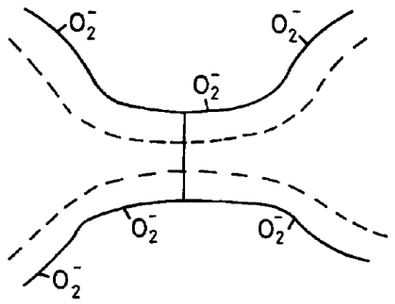

Bulk-trap limited: low oxygen partial pressures, no dependence on gas phase, logσ vs. 1/T, **slope** E_D (single activation energy)

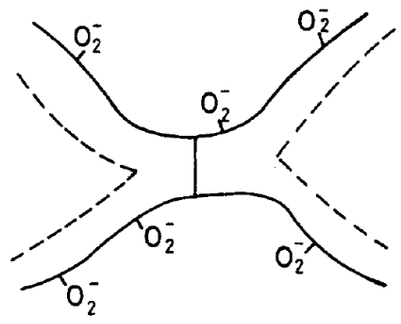

Surface-trap limited: high oxygen partial pressures; logσ vs. 1/T, dependence on oxygen partial pressure: slope $E_D \rightarrow E_S$; two or three straight line regions with **different slopes** depending on formation of increasingly stable surface species: $O_2^- < O^- < O^{2-}$

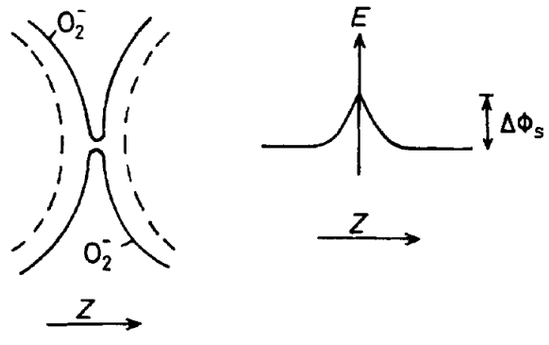

Schottky barrier: $\sigma \approx$ constant x $\exp(-e\Delta\phi_s)/k_BT$; $\Delta\phi s \sim$ (surface charge)^2 → **sigmoid plot** for change of surface charge (e.g. factor of 4 for OH^- → O^{2-}, $O^- \rightarrow O^{2-}$, $O_2^- \rightarrow 2O^-$ in dependence of T)

J. F. McAleer et al., *J. Chem. Soc. Faraday Trans. 1* **1987**, *83*, 1323-1346

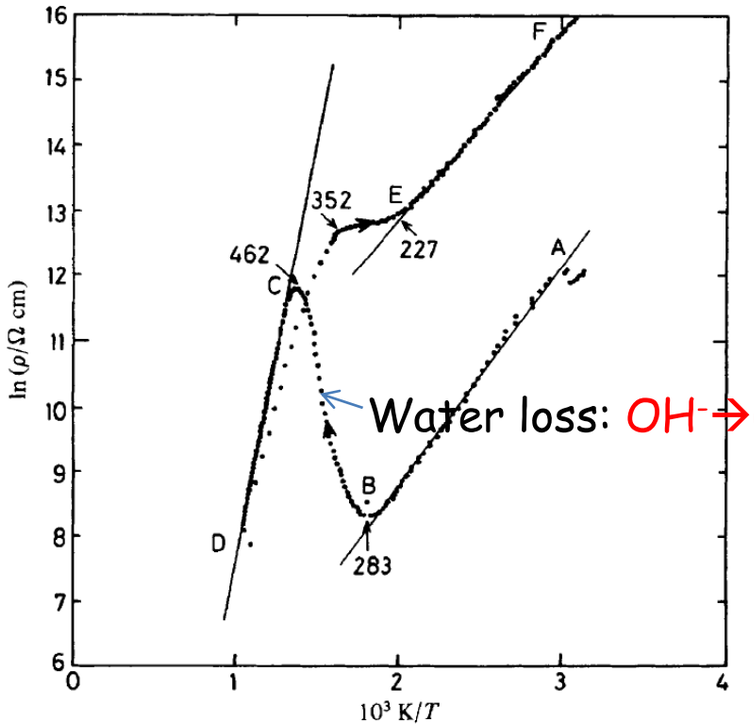

Table 2. Temperatures of physical changes in porous SnO_2

T/°C	physical change	ref.
150	desorption of O_2^-	24
160	$O_2^- - O^-$ transformation	18
227	dry slope change (point marked E)	fig. 3
280	water loss begins, minimum in air resistivity; low-temperature limit of peak in apparent gas response	fig. 3 fig. 9(*a*)
350–400	maximum in apparent gas response	fig. 9(*a*)
400	desorption of water from OH^-	24
450	high-temperature limit in apparent gas response; water loss complete; maximum in air resistivity	fig. 9(*a*) fig. 3
520	desorption of O^- or O^{2-}	24

Water loss: $OH^- \rightarrow O^{2-}$ → Schottky barrier

Fig. 3. Resistance–temperature relationship for a porous pellet of SnO_2 (FEM) in air. (i) Track ABCD: first temperature increase of moist pellet in moist or dry air. (ii) Track DCBA: reversible behaviour of pellet in moist air. (iii) Section BC: loss of moisture from moist pellet in dry air. (iv) Track DCEF: behaviour on temperature decrease, first temperature cycle in dry air. (v) Track FECD: reversible behaviour of dry pellet in dry air.

J. F. McAleer et al., *J. Chem. Soc. Faraday Trans. 1* **1987**, *83*, 1323-1346

Experimental

DC measurements

2 point DC method:

Electrical resistivity (specific electrical resistance) [Ωm]:

$$\rho = R\frac{A}{l}$$

Electrical resistance [Ωm]:

$$R = \frac{U}{I}$$

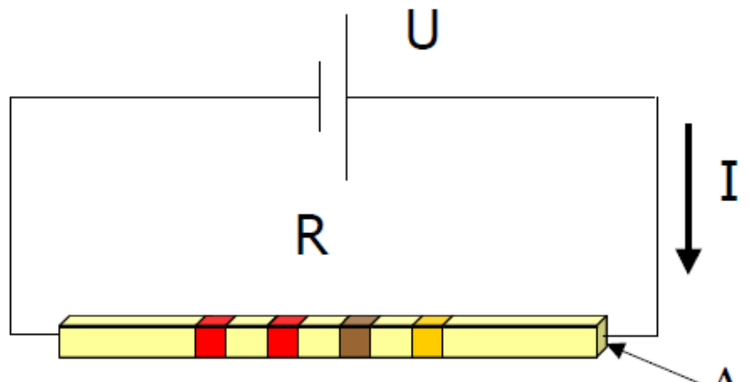

Conductivity [$(\Omega m)^{-1}$ = Mho m^{-1} = Sm^{-1}]:

$$\sigma = \frac{1}{\rho}$$

Disadvantage: contact resistance between electrodes and material surface falsifies data

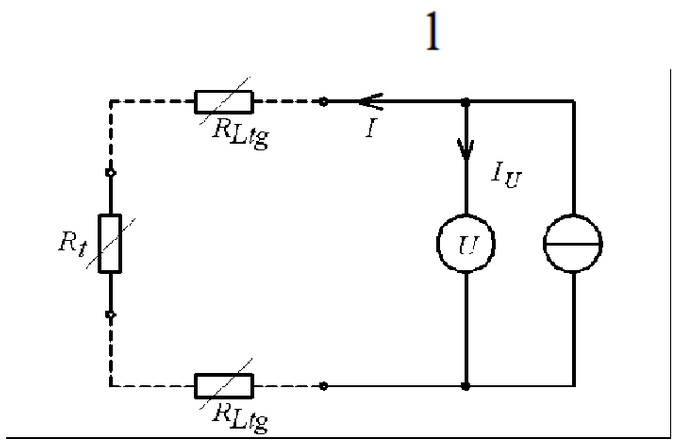

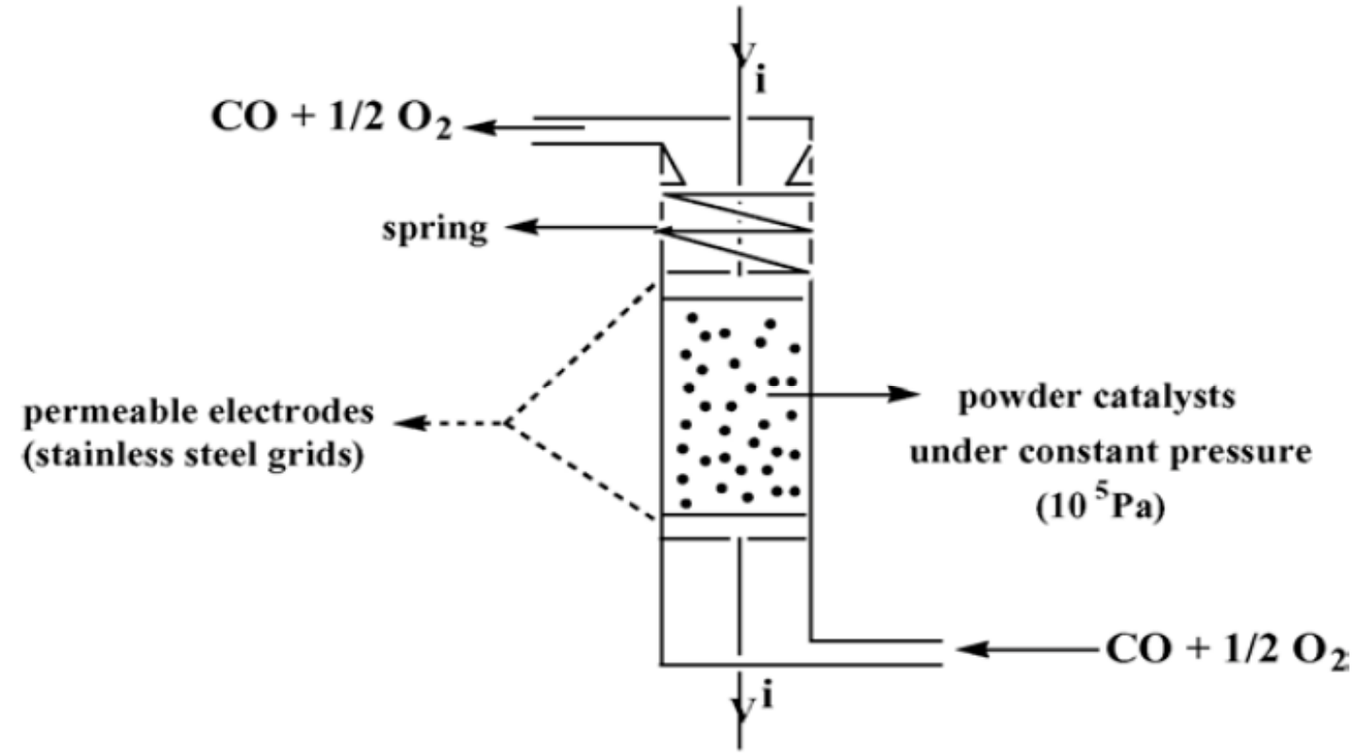

M. Breysse et al., *J. Catal.* **1972**, *27*, 275-280

DC measurements

4 point DC method:

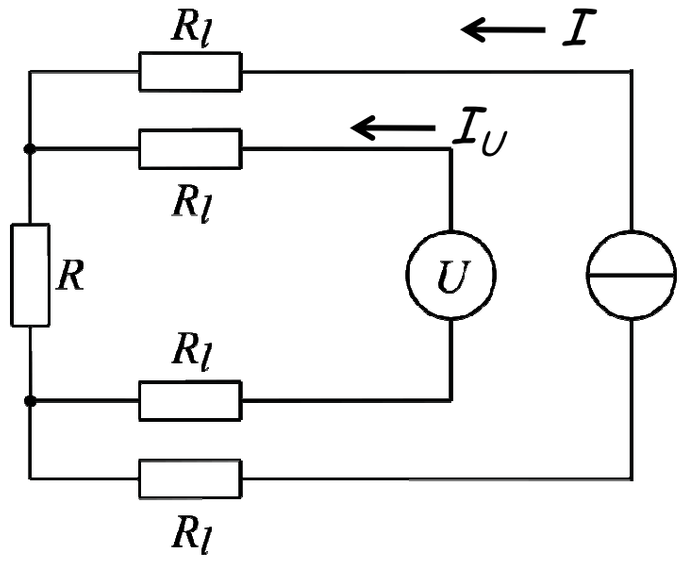

Current I is set → known

Resulting voltage U is measured

Resistance calculated with Ohm`s law

$$RI >> R_l I_U$$

Advantage: nearly no current flowing between voltmeter and contacts (measured vs. high resistance, $I_U << I$, nearly no voltage drop → R_l can be neglected)

Disadvantage: Polarization at electrode contacts

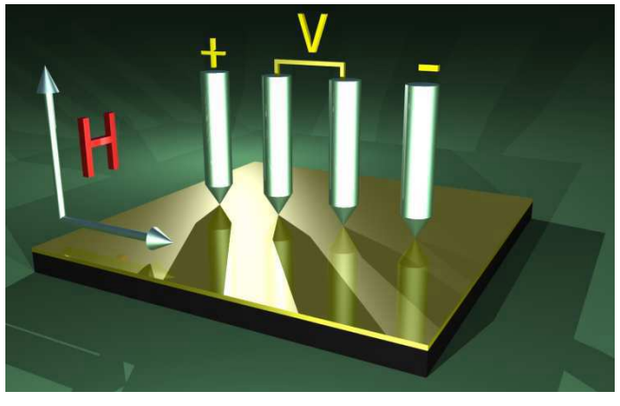

Impedance measurements (measurement at alternating voltages):

$$\boldsymbol{U}(t) = \hat{\boldsymbol{U}} e^{i(\omega t + \phi_U)}$$

$$\boldsymbol{I}(t) = \hat{\boldsymbol{I}} e^{i(\omega t + \phi_I)}$$

Impedance [Ω]: $\left|Z\right| = \dfrac{\hat{\boldsymbol{U}}}{\hat{\boldsymbol{I}}} = \sqrt{R^2 + X^2}$

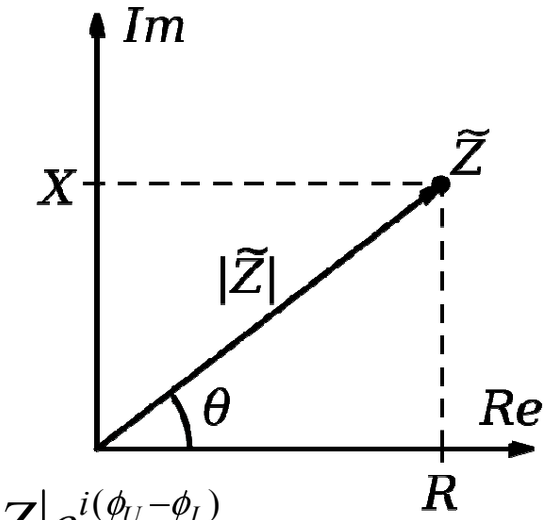

Complex impedance: $\boldsymbol{Z} = R + iX = \left|Z\right| e^{i\theta} = \left|Z\right| e^{i(\phi_U - \phi_I)}$

Resistance Reactance Phase difference between voltage and current

Ohm`s law: $\boldsymbol{U} = \boldsymbol{I}\boldsymbol{Z} = \boldsymbol{I}\left|Z\right| e^{i\theta}$

AC measurements

Impedance of an ideal resistor: $Z_R = R$

Impedance of an ideal inductor: $Z_L = i\omega L = \omega L e^{i\frac{\pi}{2}}$

Impedance of an ideal capacitor: $Z_C = \frac{1}{i\omega C} = \frac{1}{\omega C} e^{i(-\frac{\pi}{2})}$

Total impedance calculated by using rules for combining impedances in series and parallel:

Series combination: $Z_{tot} = Z_1 + Z_2 + \ldots + Z_n$

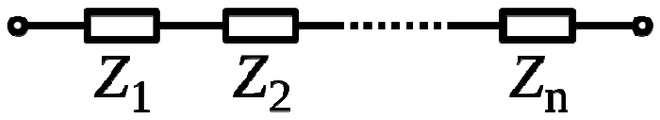

Parallel combination: $1/Z_{tot} = 1/Z_1 + 1/Z_2 + \ldots + 1/Z_n$

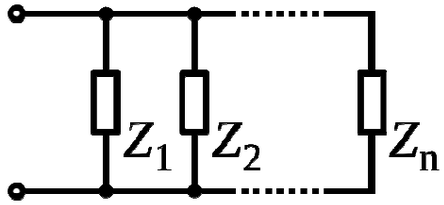

AC measurements

Catalysis Today xxx (2010) xxx–xxx

Contents lists available at ScienceDirect

Catalysis Today

journal homepage: www.elsevier.com/locate/cattod

Electrical conductivity of a MoVTeNbO catalyst in propene oxidation measured in operando conditions

M. Caldararu [a,*], M. Scurtu [a], C. Hornoiu [a], C. Munteanu [a], T. Blasco [b,**], J.M. López Nieto [b]

[a] Institute of Physical Chemistry "Ilie Murgulescu" of the Romanian Academy, Spl. Independentei 202, 060021 Bucharest, Romania
[b] Instituto de Tecnología Química, UPV-CSIC, Campus Universidad Politécnica de Valencia, Avda. Los Naranjos s/n, 46022 Valencia, Spain

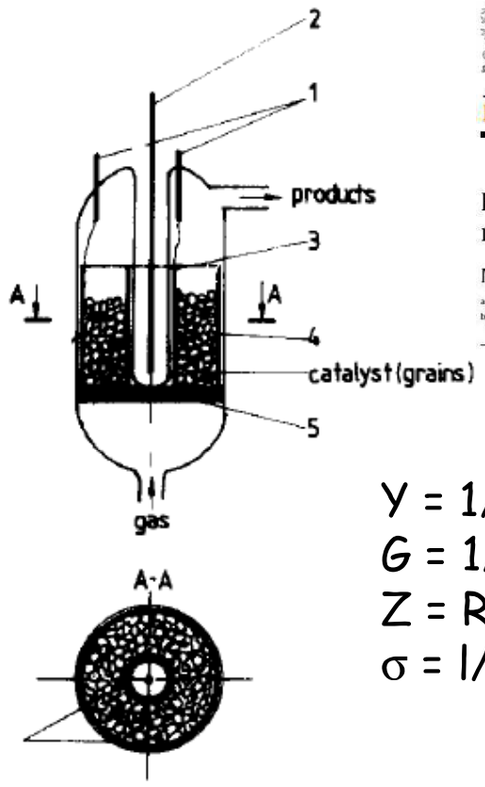

Fig. 1. Dynamic reactor providing in situ electrical conductivity and catalytic activity measurements [28]:1, tungsten contacts; 2, thermocouple; 3, tantalum cylinder (inner electrode); 4, tantalum cylinder (external electrode); 5, Pyrex glass frit.

$Y = 1/Z = G + iB$

$G = 1/R$

$Z = R + iX \rightarrow C_p = 1/X_c = -\omega C$

$\sigma = l/(R \cdot A)$

Admittance Y
Impedance Z
Conductance G
Susceptance B
Ohmic Resistance R
Reactance X
Capacity Reactance X_c
Capacity C
Conductivity s

Impedance spectroscopy

Impedance spectroscopy (IE): Sinosoidal voltage, frequency variation (typically between 10^{6} and 10^{-3} Hz)

According to Ohm's law the impedance of a sample can be calculated by complex division of the voltage and current

Looking for an "equivalent circuit" with certain impedance elements that describes best the frequency-dependent behavior of the sample

The impedance elements are related to certain physico-chemical properties, e.g. electrochemical double layer between electrode and electrolyte ions (Helmholtz layer) can be described by a capacitor

Impedance spectroscopy

Example: Investigation of redox reaction in electrolyte

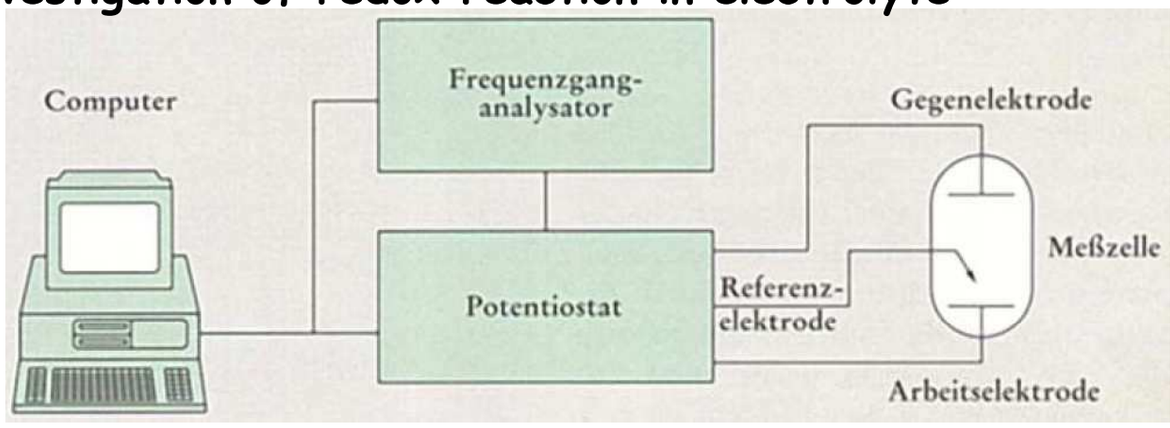

Equivalent circuit:

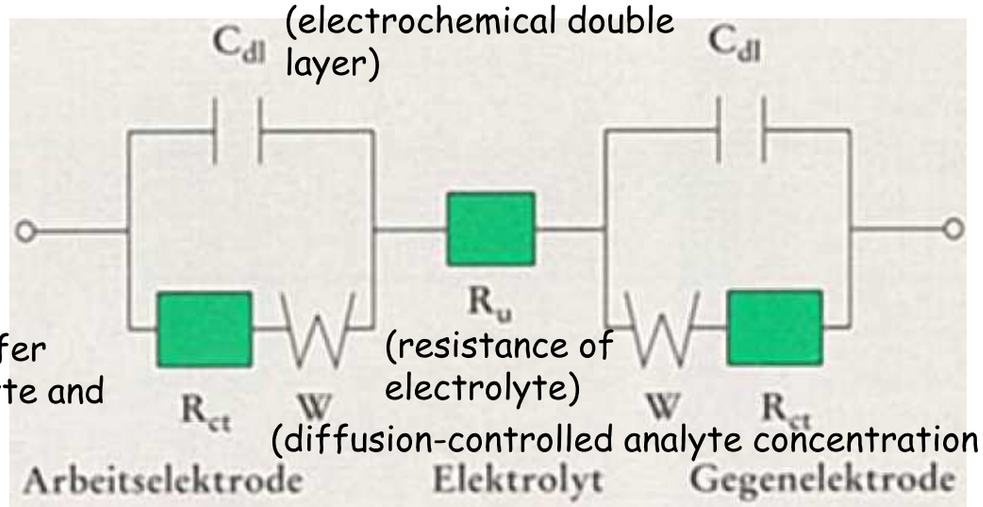

(electrochemical double layer)

(charge transfer between analyte and electrode)

(resistance of electrolyte)

(diffusion-controlled analyte concentration gradient)

D. Ende, K.-M. Mangold, *ChiuZ* **1993**, *3*, 134

Bode plot (phase angle θ vs. frequency)

e.g. oxide layer on Al

one time constant (τ = R C)

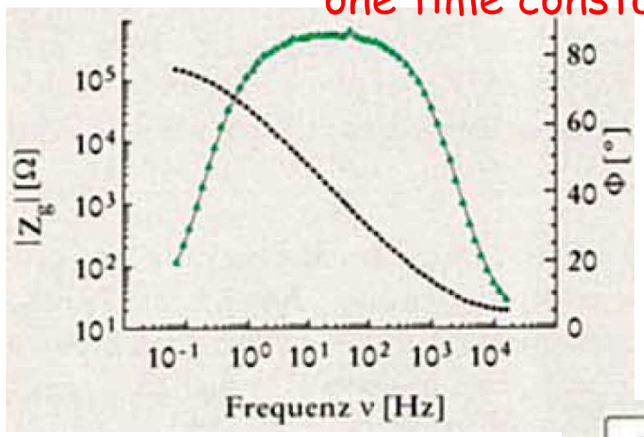

e.g. chromate layer on oxide layer on Al

two time constants

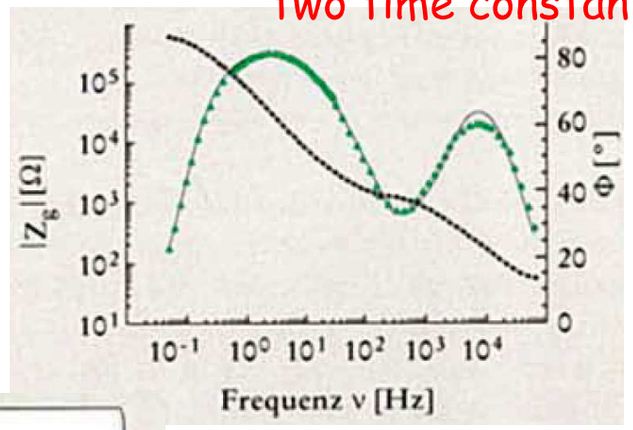

Equivalent circuit:

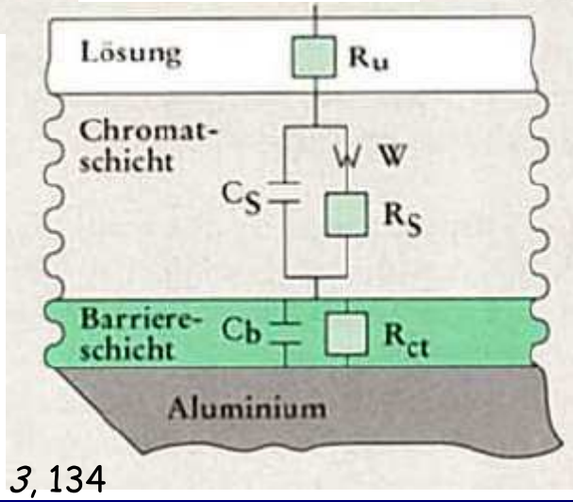

D. Ende, K.-M. Mangold, *ChiuZ* **1993**, *3*, 134

Simplified equivalent circuit for a redox reaction:

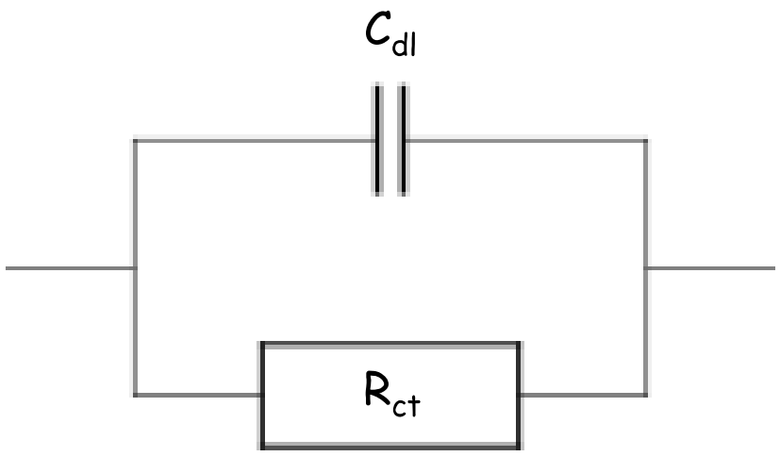

Corresponding Nyquist diagram for RC parallel circuit:

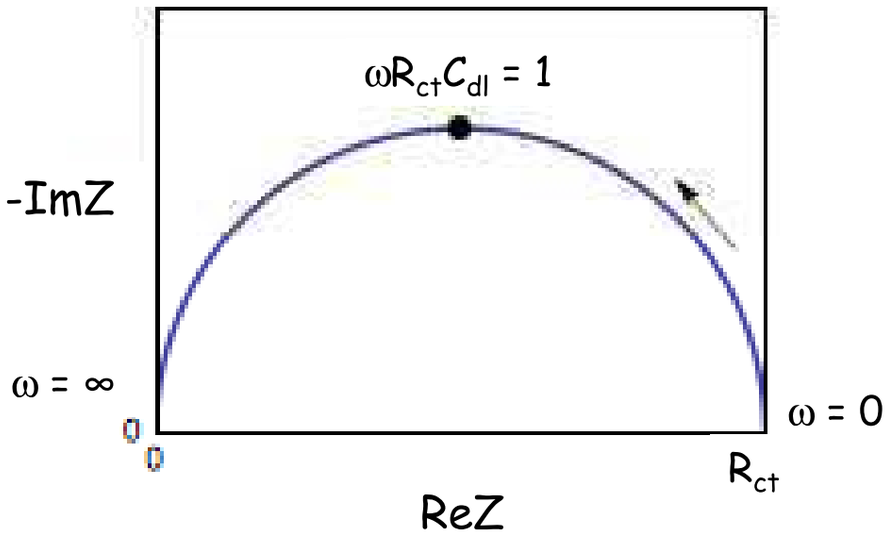

Impedance spectroscopy

IrO_2 powders as anode catalysts in water electrolysis cells (oxygen evolution reaction, OER)

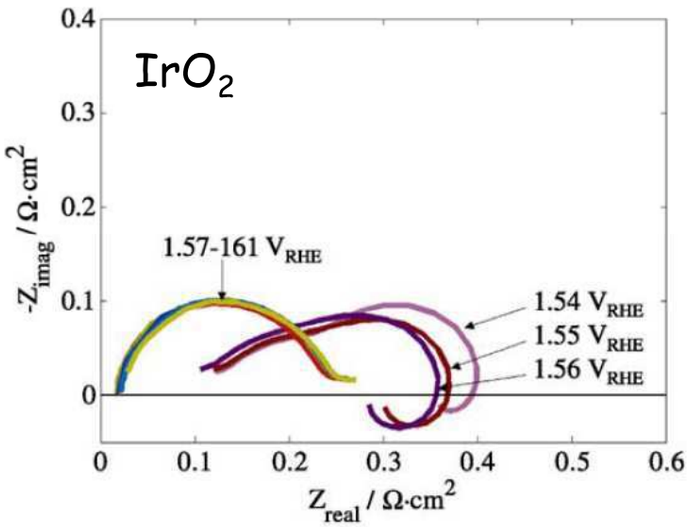

Fig. 6. Impedance of sample annealed at 440 °C as a function of potential in 10 mV steps from 1.54 to 1.61 V_{RHE} during oxygen evolution.

Two time constants, probably related to steps in OER

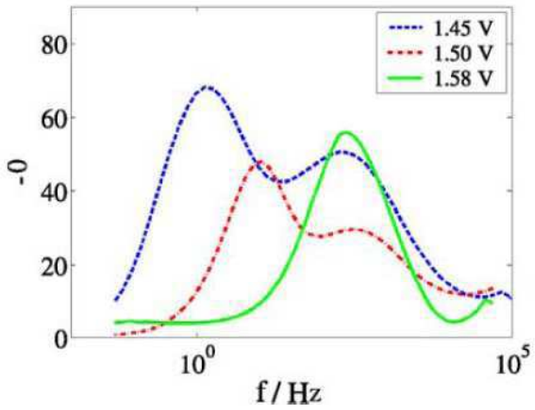

Fig. 8. Bode plot, face angle θ vs. frequency f of sample annealed at 440 °C, as function of potential.

E. Rasten et al., *Electrochim. Acta* **2003**, *48*, 3945-3952

Impedance spectroscopy

Mott-Schottky plot for a p-type SC

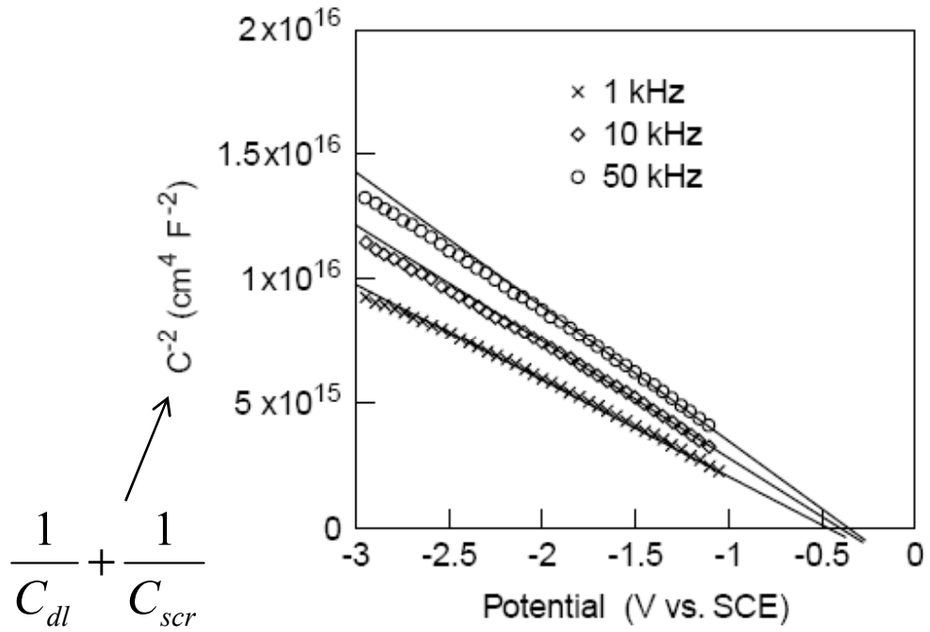

$$\frac{1}{C_{dl}} + \frac{1}{C_{scr}}$$

Mott-Schottky plot for an n-type SC

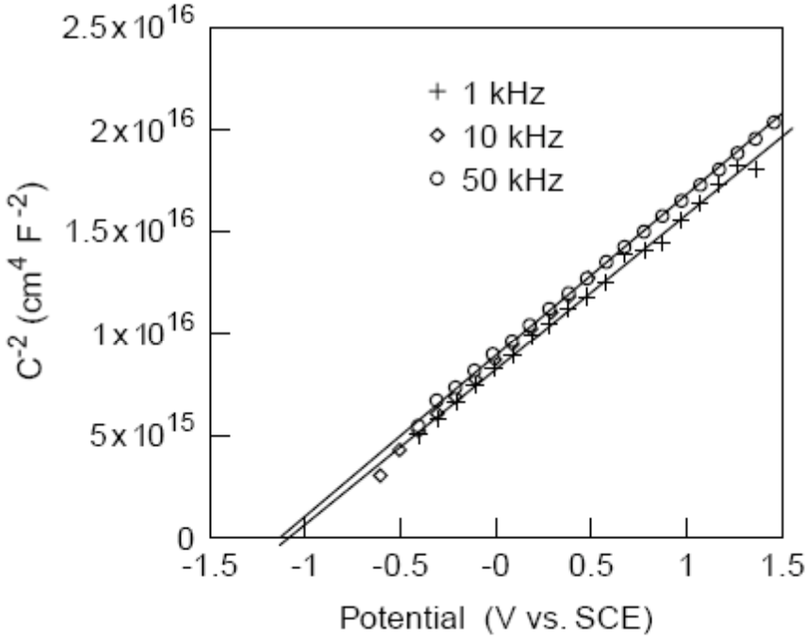

$$(C_{scr} << C_{dl} \text{ --> } \frac{1}{C_{dl}} \text{ can be neglected})$$

A. W. Bott, *Current Separations* **1998**, *17*, 87

Impedance spectroscopy

IrO_2

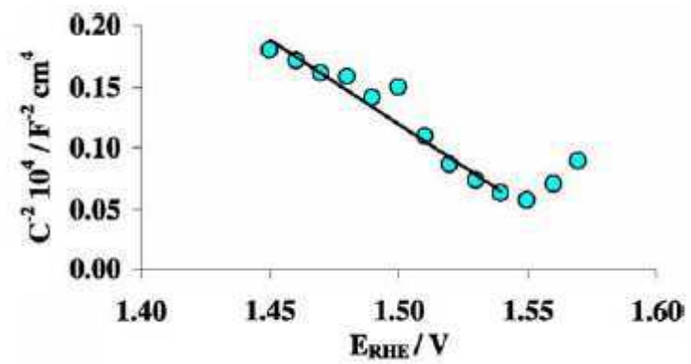

Fig. 10. Mott–Schottky plot of non-annealed sample.

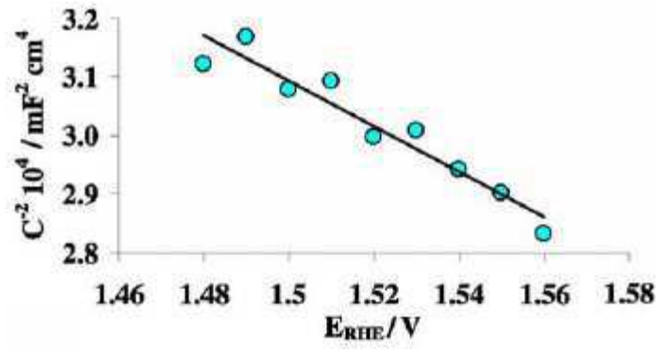

Fig. 11. Mott–Schottky plot of sample annealed at 490 °C.

Change from p-type to n-type conduction with increasing potential (e.g. due to oxidation of Ir)

Stable p-type semiconductor

E. Rasten et al., *Electrochim. Acta* **2003**, *48*, 3945-3952

Localized Impedance Spectroscopy

array of circular gold *microelectrodes* (20 μm diameter) on polycrystalline Fe-doped $SrTiO_3$

platinum contact tips

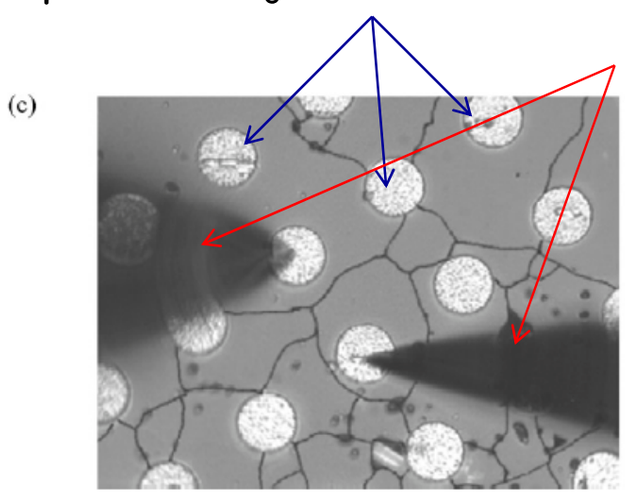

Fig. 1. (a) Electrode configuration sometimes used to perform "microelectrode" measurements. The end of a connection line is assumed to represent a micro-electrode. (b) Sketch of a model sample with extended contact electrodes and very thin highly conductive connection lines to the circular "microelectrodes". (c) Image of circular microelectrodes on a $SrTiO_3$ polycrystal contacted under the optical microscope by contact tips.

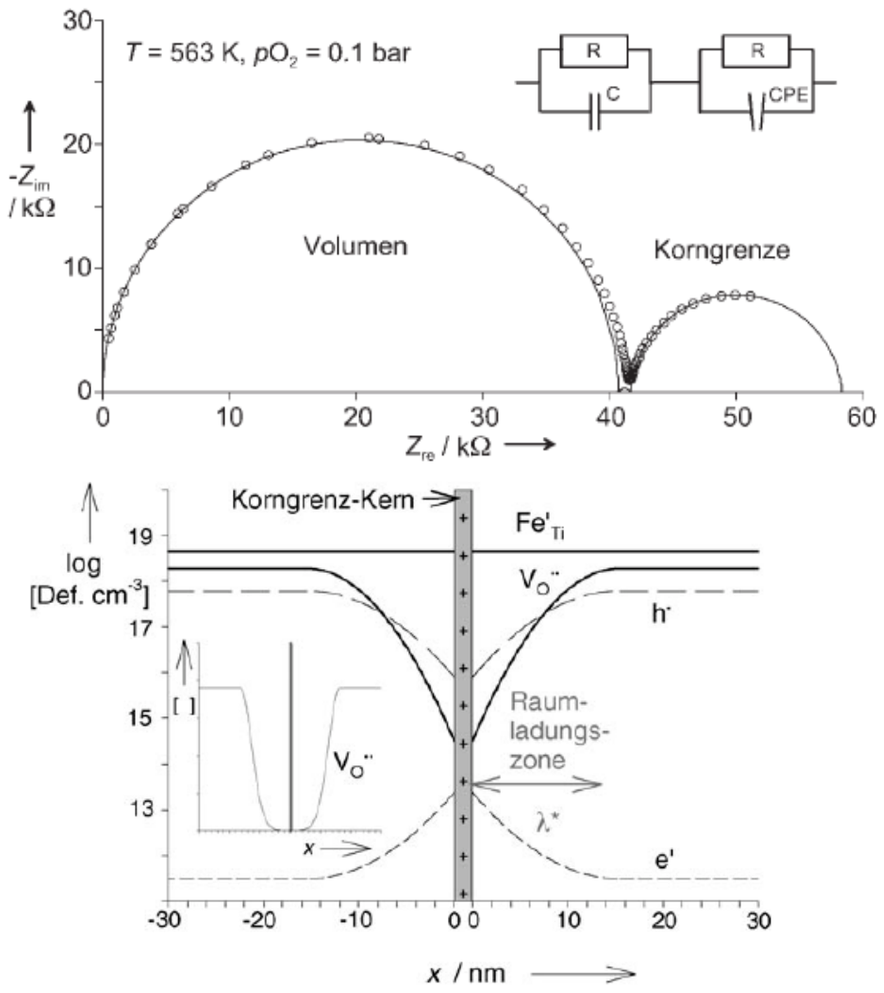

R. Merkle, J. Maier, *Angew. Chem.* **2008**, *120*, 3936-3958

Ionic/electronic conductivity

Fe-doped $SrTiO_3$ (incorporation of oxygen)

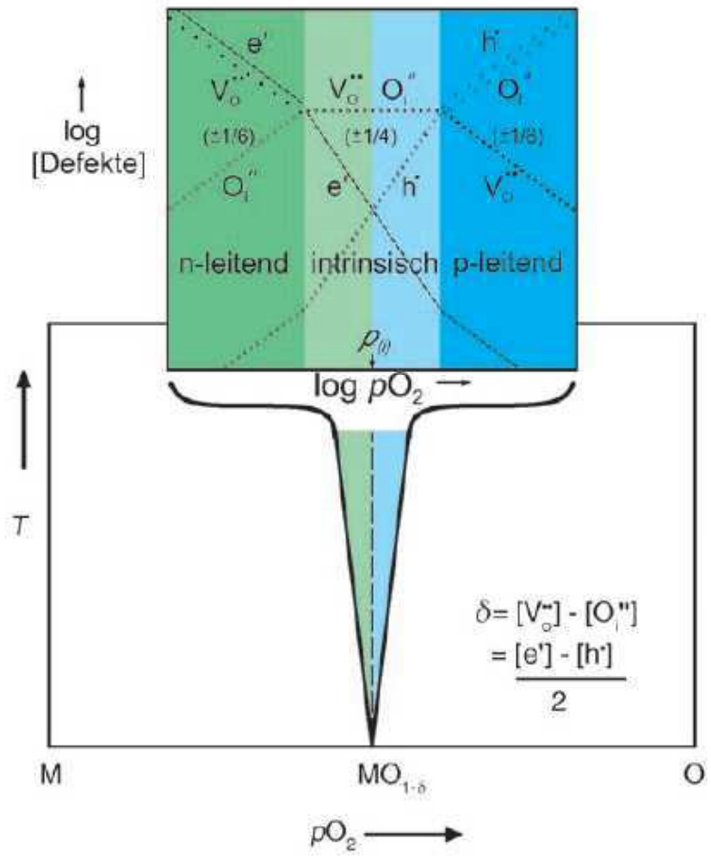

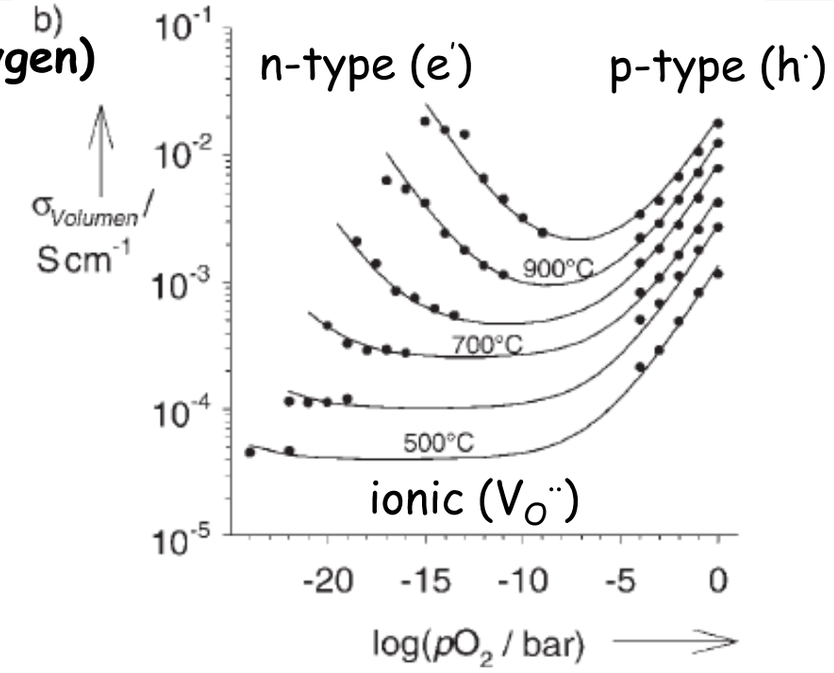

Kinetic measurements to differentiate between:

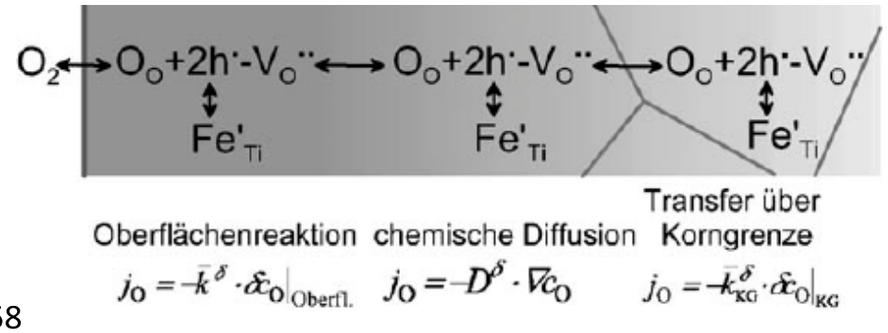

R. Merkle, J. Maier, *Angew. Chem.* **2008**, *120*, 3936-3958

Ionic conductivity

Measurement of oxygen anionic conductivity:

Oxygen ion conductor Y_2O_3/ZrO_2 can suppress hole and electron conductivity → only anion conductivity is measured

$$\sigma_{n/p} = \sigma_{total} - \sigma_{ion}$$